11-2017

Experimental Study of Low Salinity Water Flooding and Fracturing Effects in Low Permeability Carbonate Reservoir

Benny Arianto Harahap

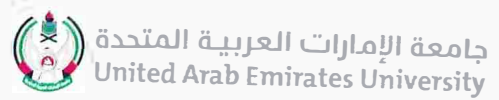Follow this and additional works at: https://scholarworks.uaeu.ac.ae/all_theses

Part of the Petroleum Engineering Commons

Recommended Citation

UAEU

جامعة الإمارات العربية المتحدة
United Arab Emirates University

United Arab Emirates University

College of Engineering

Department of Chemical and Petroleum Engineering

EXPERIMENTAL STUDY OF LOW SALINITY WATER FLOODING AND FRACTURING EFFECTS IN LOW PERMEABILITY CARBONATE RESERVOIR

Benny Arianto Harahap

This thesis is submitted in partial fulfilment of the requirements for the degree of Master of Science in Petroleum Engineering

Under the Supervision of Professor Abdulrazag Y. Zekri

November 2017

Declaration of Original Work

I, Benny Arianto Harahap, the undersigned, a graduate student at the United Arab Emirates University (UAEU), and the author of this thesis entitled *"Experimental Study of Low Salinity Water Flooding and Fracturing Effects in Low Permeability Carbonate Reservoir"*, hereby, solemnly declare that this thesis is my own original research work that has been done and prepared by me under the supervision of Professor Abdulrazag Y. Zekri, in the College of Engineering at UAEU. This work has not previously been presented or published, or formed the basis for the award of any academic degree, diploma or a similar title at this or any other university. Any materials borrowed from other sources (whether published or unpublished) and relied upon or included in my thesis have been properly cited and acknowledged in accordance with appropriate academic conventions. I further declare that there is no potential conflict of interest with respect to the research, data collection, authorship, presentation and/or publication of this thesis.

Student's Signature: _____   Date: _27 / 12 / 2017_

Advisory Committee

1) Advisor: Prof. Abdulrazag Y. Zekri

Title: Professor

Department of Chemical and Petroleum Engineering

College of Engineering

2) Co-advisor: Dr. Hazim Al Attar

Title: Associate Professor

Department of Chemical and Petroleum Engineering

College of Engineering

Approval of the Master Thesis

This Master Thesis is approved by the following Examining Committee Members:

1) Advisor (Committee Chair): Prof. Abdulrazag Y. Zekri

   Title: Professor

   Department of Chemical and Petroleum Engineering

   College of Engineering

   Signature _____   Date 11/12/2017

2) Member (Coordinator, Master Program): Dr. Gamal Alusta

   Title: Assistant Professor

   Department of Chemical and Petroleum Engineering

   College of Engineering

   Signature _____   Date 11/12/2017

3) Member (External Examiner): Prof. Ezeddin Shirif

   Title: Professor

   Department of Petroleum System Engineering

   Institution: University of Regina, Canada
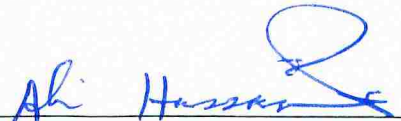
   Signature _____   Date 11/12/2017

This Master Thesis is accepted by:

Dean of the College of Engineering: Professor Sabah Alkass

Signature _____ Date _14/12/2017_

for Dean of the College of Graduate Studies: Professor Nagi T. Wakim

Signature ___Ali Hassan___ Date _27/12/2017_

Copy _8_ of _9_

Abstract

In past decades, there were numerous research works demonstrated that salinity alteration of injected water could enhance the oil recovery. Low salinity water (LSW) injection is a type of Enhanced Oil Recovery (EOR) method which attracts the industrial and researchers because of its simplicity to use the implications, environment-friendly nature, and less cost. In addition to, hydraulic fracturing, also known as hydraulic stimulation, is another EOR method that improves hydrocarbon flow by creating fractures in the Low Permeability Formation (LPF) that connects the reservoir and wellbore. Fractures will increase the permeability of reservoir and give the flow path for hydrocarbon to be produced. The main objective of this study is to compare between low salinity injection and fracturing as a recovery technique for LPF. The LSW flooding tests conducted, with several salinity concentrations (157,662; 72,927; 62,522; 6,252; and 1,250 ppm), in both artificially fractured and non-fractured carbonate cores that filled with crude oil. The properties of injected water and its dilutions (LSW) have been thoroughly investigated in the laboratory. The crude oil and low permeability chalky limestone core samples (permeability ranges from 0.01 - 1.2 millidarcy) were selected from oil fields in the United Arab Emirates (UAE). The experiment shows that seawater (SW) diluted ten times (6,252 ppm) is the optimum salinity in enhancing the oil recovery for selected reservoir condition. Additional oil recoveries for SW and SW diluted ten times are 4.9% and 12.7% respectively. On the other hand, the fractured system produced up to 7.4% incremental oil recovery more than the non-fractured system. Moreover, a combination of fracturing and LSW(6,252 ppm) improved the best recovery by 17.7% of remaining oil in place over the formation brine injection. Fines migration and dissolution that may lead to wettability alteration were investigated as the reason behind LSW flooding. Results of this study could be used as an additional reference in selecting most efficient EOR method that could be applied by the UAE and worldwide companies to enhance oil recovery for low permeability carbonate reservoir.

Keywords: Enhance oil recovery, low permeability carbonate reservoir, low salinity waterflooding, fracturing.

Title and Abstract (in Arabic)

دراسة تجريبية عن مياه الفيضانات ذات ملوحة منخفضة وتأثيرات التصدع في انخفاض نفاذية كاربونات احتياطي النفط

الملخص

في العقود الماضية كان هناك العديد من الأعمال البحثية التي أثبتت أن تغير الملوحة في المياه المحقونة يمكن أن يعزز استعادة النفط. إن حقن المياه الملوحة منخفض (LSW) هو نوع من أساليب نمز بز استعادة النفط (EOR) المحسن التي تجذب الصناعيين والباحثين بسبب بساطته لاستخدام الآثار، والطبيعة صديقة للبيئة، وأقل تكلفة. وبالإضافة إلى ذلك، فإن التكسير الهيدروليكي، المعروف أيضا باسم التحفيز الهيدروليكي، هو طريقة أخرى EOR يحسن تدفق الهيدروكربون من خلال خلق كسور في تكوين النفاذية المنخفضة (LPF) الذي يربط الخزان وحفرة البئر. الكسور سوف تزيد من نفاذية الخزان وصنع مسار لانتاج الهيدروكربون. الهدف الرئيسي من هذه الدراسة هو مقارنة بين انخفاض الملوحة الحقن والتكسير كطريقة استرداد LPF. وأجريت اختبارات الفيضانات في LSW مع عدة تركيزات ملوحة (157،662، 72،927، 62،522، 6،252 و 1،250 جزء في المليون)، في كل من النوى الكربونية المتصدعة المصنعة وغير المتصدعة والمملوء بالنفط الخام. وقد تم فحص خصائص المياه المحقونة وتراكيزها المنخفضة بدقة في المختبر. تم اختيار النفط الخام وعينات الحجر الجيري الطباشيري ذو نفاذية منخفضة (نفاذية تتراوح بين 0.01 - 1.2 ميليدارسي) من حقول النفط في الإمارات العربية المتحدة. وتبين التجربة أن مياه البحر (SW) المخففة عشر مرات (6،252 جزء في المليون) هي الملوحة المثلى في تعزيز استعادة النفط لحالة خزان مختارة. استخلاص النفط إضافية ل SW و SW المياه البحر المخفف عشر مرات هي 4.9٪ و 12.7٪ على التوالي. ومن ناحية أخرى، أنتج النظام المكسور ما يصل إلى 7.4٪ من عمليات استخراج الزيت الإضافية أكثر من نظام غير مكسور. وعلاوة على ذلك، فإن الجمع بين تاماكم الحقن قوية و LSW (6،252 جزء في المليون) تحسن أفضل استعادة بنسبة 17.7٪ من النفط المتوافر في على تشكيل حقن محلول ملحي. وقد تم التحقيق في هجرة الا غرامات وخلا لها والتي قد تؤدي إلى تعديل wettability كسبب LSW. ويمكن استخدام نتائج هذه الدراسة كمرجع إضافي في اختيار الطريقة الأكثر كفاءة لليورانيوم التي يمكن تطبيقها من قبل الشركات الإماراتية والعالمية لتعزيز استرداد النفط لخزان الكربونات منخفض النفاذية.

مفاهيم البحث الرئيسية: تعزيز استرداد النفط، انخفاض نفاذية كربونات الخزان، منخفضة الملوحة فيضان الماء، التكسير.

Acknowledgements

Dedication

I dedicate this to my beloved parents and sisters,
who always be at the past, present and future.

Table of Contents

List of Tables

List of Figures

List of Abbreviations

ADNOC Abu Dhabi National Oil Company

EOR Enhance Oil Recovery

FW Formation Water

HF Hydraulic Fracturing

IFT Interfacial Tension

LPCR Low Permeability Carbonate Reservoir

LSW Low Salinity Water

LSWF Low Salinity Water Flooding

MBOED Million Barrels of Oil Equivalent per Day

PV Pore Volume

RF Recovery Factor

SW Seawater

OOIP Original Oil In Place

UAE United Arab Emirates

UAEU United Arab Emirates University

Chapter 1: Introduction

1.1 Overview

As global population is projected to increase by 1,772 million from 2015 into reach 9,078 million in 2040, total primary energy demand is forecasted to be increased by 40% in the period to 2040 to reach 382 Million Barrels of Oil Equivalent per Day (MBOE/D). Energy mix continues to see fast growth for renewables, but 53% of the world's energy needs will still be satisfied by oil and gas in 2040 (Ban et al., 2016).

The technology and technique for improving the hydrocarbon production and field development still be mandatory to be developed in order to fulfil future people's energy demand. Enhance Oil Recovery (EOR) techniques present solutions to meet the increasing demand for energy. Since worldwide oil and gas fields are heterogeneous of varying degrees, thus the obstacles and properties will be different from one field to another. Research and development should be conducted for each particular case to give a better understanding and more alternative options.

1.2 Background

More than 60 % of the world's petroleum is produced from carbonate reservoirs. Unlike the sandstone reservoirs which are relatively homogenous, carbonate reservoirs (limestone or dolomite) contain highly varying properties (e.g., permeability, porosity, flow mechanisms, etc.) within a small area of the reservoir, making them difficult to characterize.

Low permeability carbonate reservoir (LPCR) was considered uneconomical because of low flow rate and longer pay out time. However, due to increasing of energy

demand, nowadays, research and developments are conducted to be able to produce and improve the hydrocarbon recovery from these type of reservoir.

In past decades, numerous research work has been demonstrated that salinity alteration of injected water could enhance the oil recovery. Low salinity water (LSW) injection is a type of Enhanced Oil Recovery (EOR) method which attracts the industry and researchers because of its simplicity to implement, environment-friendly nature, and cost-effectiveness.

In addition, hydraulic fracturing, also known as hydraulic stimulation, is known to improve hydrocarbon flow from reservoir matrix into the wellbore by creating fractures in the Low Permeability Formation (LPF). Induced fractures create low resistance flow path for hydrocarbon and improve wells productivity.

1.3 Statement of the Problem

Many previous experiments of LSWF (for example: Al-Harrasi et al. (2012), Zahid et al. (2012), Zekri et al. (2012), and Al-Attar et al. (2013)) were successful in improving the oil recovery from the moderate to high permeability of carbonate reservoirs. Alameri et al. (2015) proved that LSFW could be used in LPCR condition. However, very few research conducted in LSWF for LPCF, so this thesis could confirm and give more details for the specified condition.

Fractures may be present in the reservoir in the form of natural network or induced and oriented. For LPF, fractures will be artificially made by hydraulic fracture technique. The latter technique is a common technique used by the oil and gas companies for LPF condition, nowadays.

In order to get a better resolution and efficient ways to enhance the oil recovery from the LPCR, this thesis addresses the effectiveness of the two, Low Saline

Waterflooding (LSWF) and induced fracturing, and the combination. To achieve the objective, experiments were designed to flood tight core samples, with and without fracture, using various brines.

1.4 Relevant Literature

An oil field encounters several recovery stages during the oil production process. Stosur et al. (2013) explain that there will be 3 recovery stages during the lifetime of oil production, primary, secondary and tertiary which reflect and describe the natural progression of oil production from its inception to the point where economic production is no longer feasible.

Initially, at the early time of production, oil flows to the surface as a result of the natural energy of the reservoir itself. These natural forces are driven by one or combination of these several factors: pressure decline, the evolution of dissolved gas, expansion of gas cap, or the influx of natural water.

In the secondary recovery stage, as reservoir pressure drops due to the oil production earlier, drive energy is depleted and the production could be uneconomic. Water or gas will be injected from the injection well as an energy support and keep the oil production to be economical. The process depends mainly on physical displacement to recover additional oil.

Once the water or gas injection is not supporting enough, the remaining oil can be enhanced by vary of tertiary recovery techniques: addition of heat, chemical interaction between the injected fluid and the reservoir oil, mass transfer, and/or changing of oil or reservoir properties in such a way that the process facilitates oil movement through the reservoir. Tertiary recovery processes generally include

thermal, chemical, gas miscible and microbial and these processes referred to as EOR processes.

1.4.1 Low Salinity Waterflooding

LSWF has widely been practiced in improving the oil recovery due to simplicity, availability of the water sources and relatively cheaper than other practical techniques. LSWF studies in sandstone reservoir have been started from 1990, initiated by Morrow who analyzed the wettability effect on oil recovery. Morrow and his colleagues developed the study. Jadhunandan and Morrow (1995) found that wettability is affecting on waterflood recovery. In 1997, Tang and Morrow concluded that salinity of waterflooding could be enhancing the oil recovery by experimental work, then started from this publication, many researchers conducting the research on LSWF in order to get the better explanation and mechanism behind this technique.

Bagci et al. (2001) started the investigation of LSWF on carbonate cores (limestone) since previous experiments used sandstone cores. They showed that decreasing the salinity of water injection is applicable to EOR in carbonate rocks.

Al-Harrasi et al. (2012) conducted low-salinity waterflood experiments using different carbonate cores. Injected synthetic brine was mixed with distilled water in four ways making varying concentrations (dilution brine was mixed twice, 5 times, 10 times, and 100 times). In conclusion, using coreflooding and spontaneous imbibition experiments, they reported an increase of 16-21% in oil recovery.

Zahid et al. (2012) stated that LSWF is giving the incremental of oil recovery for carbonate rock when the experiments were running in high-temperature condition while in the ambient condition the LSWF did not give any effect at all. They assumed that, in

high-temperature condition, migration of fines or dissolution effects may have occurred due to the increase in pressure drop, and may contribute to the increase in oil recovery.

Moreover, Zekri et al. (2012) performed various experiments changing contact angles as a function of time. Several types of brine injection concentrations were used in the experiment to examine the effect of salinity in oil recovery, while different sulfate concentrations. They concluded the main mechanism of increasing recovery in both limestone and sandstone formations is the wettability alteration.

In addition to, Al-Attar et al. (2013) investigated coreflood experiments involving low-salinity waterflood in UAE carbonate reservoirs. Various dilutions of seawater were used in order to examine the effect of low-salinity water based on brine salinity and ionic compositions. Moreover, they performed wettability alteration using contact angle measurements, and interfacial tension measurements were also determined. In result, they concluded an oil recovery increased during LSWF. As the sulfate concentration increased the oil recovery increase. However, when the concentration reached a high level it had a negative effect on recovery.

An experimental and numerical modeling of LSWF study that specified on LPCR condition was conducted by Alameri et al. (2015). They conducted coreflooding, interfacial tension and contact angle analysis during the LSFW. They confirmed that LSFW could be used in LPCR condition as well. The improvement of oil recovery caused by the wettability alteration more to water wet.

Simulation on LSFW study on carbonate fractured reservoir performed by Wu (2009) accepted that lower salinity water injection would give higher oil recovery rate than high salinity.

1.4.2 Low Salinity Waterflooding Mechanism

Since 1999, there are seventeen mechanisms of LSWF have been proposed by various researchers by conducted many experiments and conditions (Sheng, 2014), as follows: (1) fine migration; (2) mineral dissolution; (3) limited release of mixed-wet particles; (4) increased pH effect and reduced interfacial tension (IFT); (5) emulsification/snap-off; (6) saponification; (7) surfactant-like behavior; (8) multicomponent ion-exchange (MIE); (9) double layer effect; (10) particle-stabilized interfaces/lamella; (11) salt-in effects; (12) osmotic pressure; (13) salinity shock; (14) wettability alteration (more water-wet); (15) wettability alteration (less water-wet); (16) viscosity ratio; and(17) end effects. However, Sheng concluded that most likely, several mechanisms work under a specific condition. And different mechanisms work in different conditions. Among the proposed mechanisms, the probably most plausible mechanism is wettability alteration. This mechanism can be used to explain more cases because wettability can be changed from oil-wet to water-wet, or from oil-wet to inter-mediate or mixed wet. In either way, oil recovery factor could be improved.

Kilybay et al. (2017) proposed that at least there are 4 possible mechanisms behind the LSWF on carbonate formation, wettability alteration, rock dissolution, electric double layer effect and IFT reduction.

1.4.2.1 Wettability alteration

Wettability is defined as the tendency of one fluid to spread on or adhere to a solid surface in the presence of other immiscible fluids (Ahmed T., 2000). This spreading tendency can be expressed more conveniently by measuring the angle of contact at the liquid-solid surface. This angle, which is always measured through the liquid to the solid, is called the contact angle θ as shown in Figure 1.

The wettability of reservoir rocks to the fluids is essential because the distribution of the fluids in the porous media is a function of wettability. Because of the attractive forces, the wetting phase tends to occupy the smaller pores of the rock and the non-wetting phase occupies the more open channels. Also, wetting phase fluid often has low mobility, while non-wetting phase fluid is often the most mobile fluid (Ahmed T., 2000).

Since worldwide carbonate reservoirs are believed to have mixed wettability or to be oil wet, wettability alteration to be more water wet will be resulting in increasing oil recovery (Alotaibi et al., 2010).
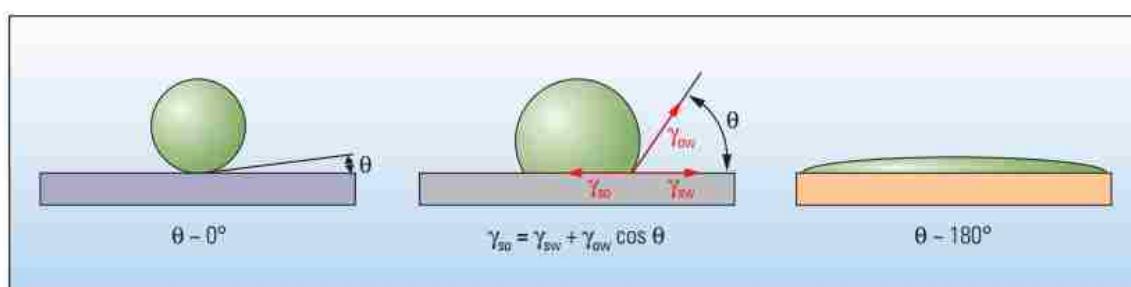
Figure 1: Contact angle as an indicator of wettability
(Abdallah et al. 2007)

In Figure 1, an oil drop (green) surrounded by water (blue) on a water-wet surface (left) forms a bead. The contact angle θ is approximately zero. On an oil-wet surface (right), the drop spreads, resulting in a contact angle of about 180°. An intermediate-wet surface (center) also forms a bead, but the contact angle comes from a force balance among the interfacial tension terms, which are γ_{so} and γ_{sw} for the surface-oil and surface-water terms, respectively, and γ_{ow} for the oil-water term.

Kilybay et al. (2017) believed that main reason for altering the wetting surface of the rock surface is the multicomponent ionic exchange. In carbonate rocks, the

potential determining ions such as Ca^{2+}, Mg^{2+}, and SO_4^{2-} are the driving ions in changing the wettability as shown in Figure 2.
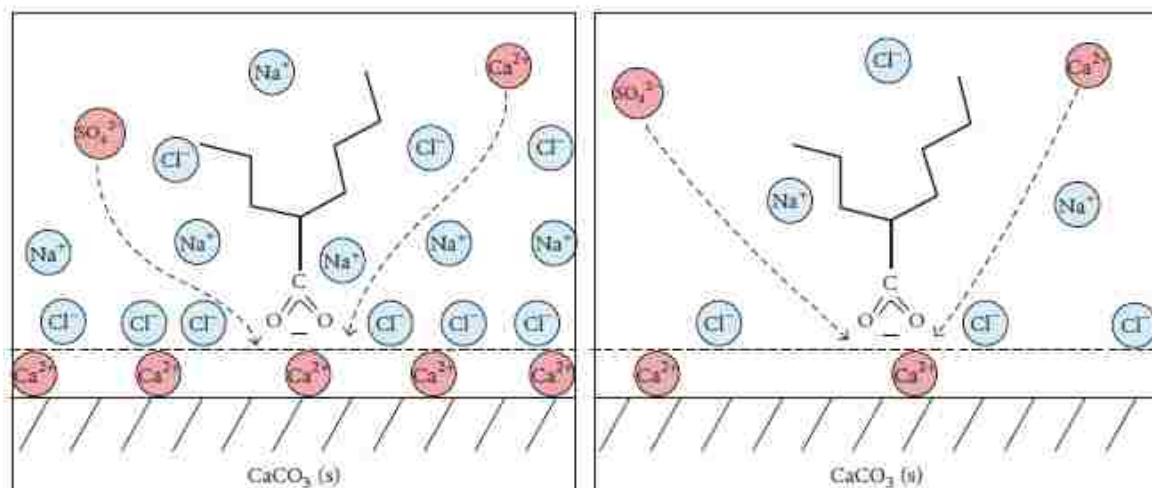
Figure 2: Schematic of wettability alteration principle by injecting sea water (Kazankapov, 2014)

Yi and Sarma (2012) concluded that multi ionic exchange concept in carbonate reservoirs is quite different to that in sandstone reservoirs. In sandstone rocks, the cation exchange happens in rock/brine/oil systems, while in carbonate rocks it is an anionic exchange between rock and brine (Figure 2). In carbonate rocks, multi ionic exchange works mainly due to the potential determining ions (Ca^{2+}, Mg^{2+}, and SO_4^{2-}). The rock surface adsorbs SO_4^{2-}, which is also coadsorbed by Ca^{2+} and Mg^{2+} ions, while carboxylic acids desorb from rock surface as potential determining ions replace them. As a result of this ionic exchange, the rock surface will turn to a more water-wet state.

1.4.2.2 Rock dissolution

Austad et al. (2010) found that low salinity water in carbonates works by

decreasing the calcium concentration in produced brine. This change causes fines migration and calcium carbonate dissolution to establish an equilibrium within brines. It is a proven phenomenon that the component of oil will be released from the rock surface as a result of rock mineral dissolution.

By lowering the salinity of injected brine to the carbonate rocks, the brines equilibrium may be disturbed that might lead to fines migration and calcium carbonate dissolution (Figure 3); as a result of that, the components of the oil could be released from rock surface (Figure 4) and change in wettability of the rock towards more water-wet condition may happen. Moreover, as a result of rock dissolution, dissolved minerals will be transported through the formation and later precipitate and might block some pore throats.
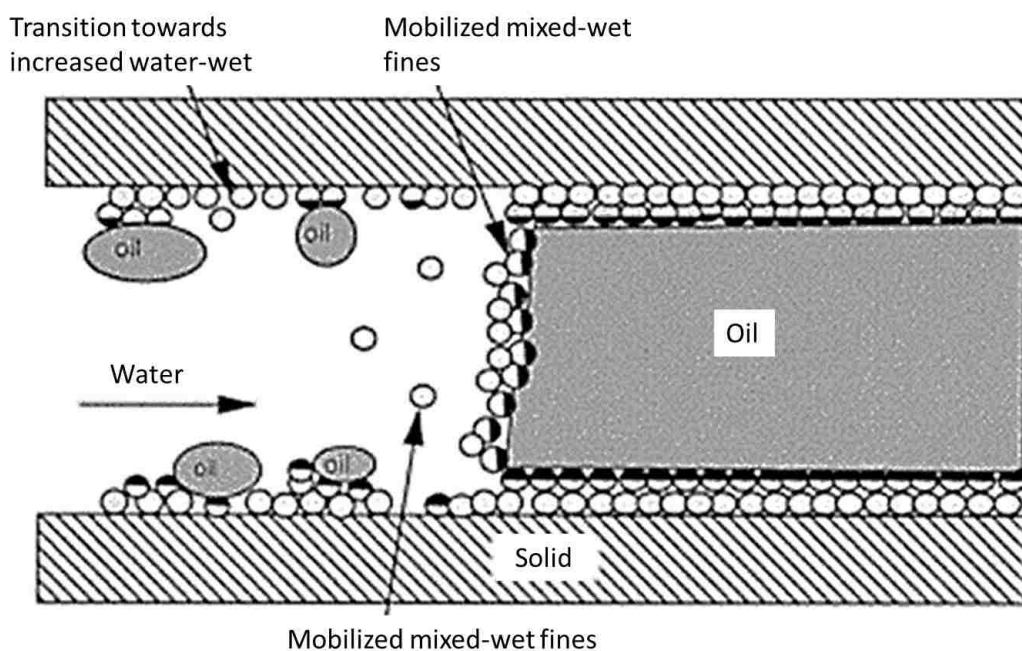
Figure 3: Low saline water dissolve fines carbonate particle
(Tang and Morrow, 1999)
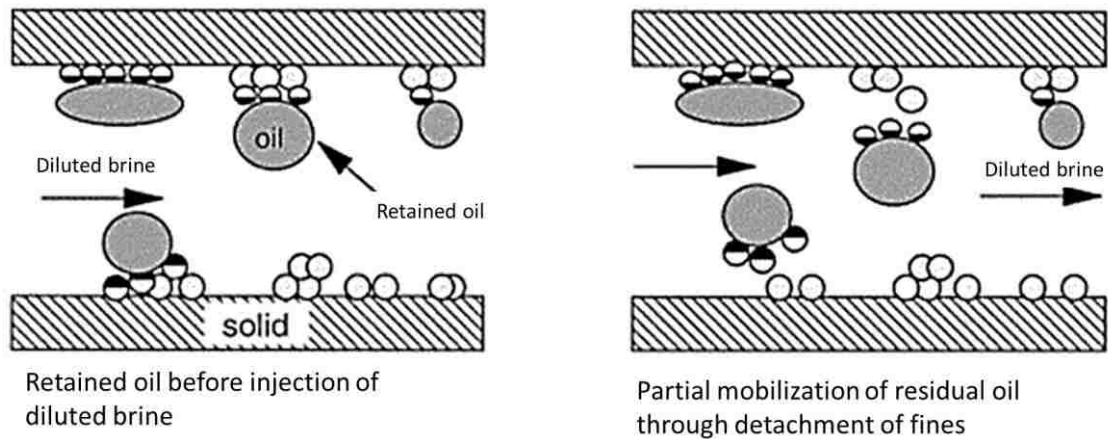
Figure 4: Trapped oil mobilization during LSWF
(Tang and Morrow, 1999)

When some of the pore throats get blocked, the flow path would change to another flow unit in the reservoir towards unswept zones and improve the microscopic sweep efficiency. This behavior in the formation is possibly the main mechanism behind improved oil recovery by low salinity water.

1.4.2.3 Electric double layer effect

The rock surface has an electrical charge and it generates an electrical field when it contacts water and creates two layers on its surface. First, it attracts oppositely charged ions, which are called counter ions, and creates a charged surface. Second, due to the thermal motion, another layer forms by these counter ions which is called a diffuse layer outside the charged surface. These two layers of diffuse and charged surfaces are called electrical double layers (EDL), which establishes an electrical neutral environment (Tadros, 1987). A schematic of electric double layer is given in Figure 5.
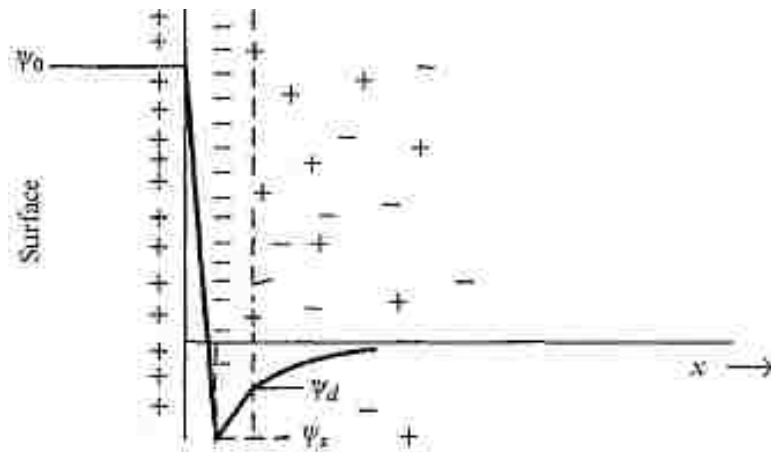
Figure 5: Example of electric double layer, where anions strongly attached to positively charged rock surface (Tadros, 1987)

Electric double layer could be the main contributor to low salinity water flood recovery due to the reduction of brine's ionic strength, the wettability tends to change to more water wet state.

1.4.2.4 IFT reduction

Teklu et al. (2014) conducted several corefloods on carbonate and sandstone cores to investigate the combined effects of injecting low salinity water and CO_2 on oil recovery. Results showed a further decrease in both contact angle and IFT using the combined CO_2 and low salinity water. Al-Quraishi et al. (2015) conducted interfacial tension measurements between oil and different brines using pendant drop tensiometer at reservoir conditions. With decreasing salinity of brines by dilution up to 10 times, the interfacial tension between oil and brine reduced to about 6 units which is not significant enough to be a dominant mechanism for low salinity water flooding.

Many of the researchers believe that, by changing the ionic composition of injecting brine, the capillary forces in the core will be affected and result to alter the contact angle and wettability. Hence, more future research is needed for role of IFT reduction to

the improving oil recovery.

1.4.3 Fracturing

A reservoir fracture is a naturally occurring macroscopic planar discontinuity in the rock due to deformation or physical diagenesis (Nelson, 2001). Nelson explained that open fractures, no deformational or diagenetic material filling the width between the walls of the fracture, greatly increase reservoir permeability parallel to the fracture plane. However the fracture orientation has an important role, it will have little or no effect on fluid flow perpendicular to the fracture plane (Figure 6).
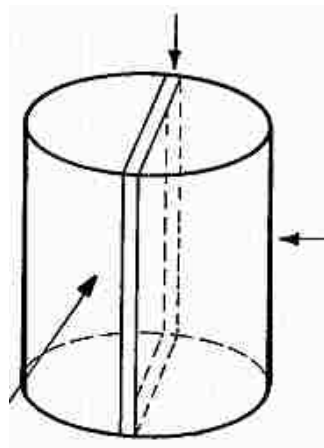
Figure 6: Example of 3-D whole-core permeability associated with an open fracture (Nelson, 2001)

Creating artificial fractures in the reservoir is known as Hydraulic Fracturing (HF). HF is a method by which access to crude oil and natural gas trapped in impermeable and hard to reach geologic formations is achieved (Speight, 2016).

The hydraulic fracturing process involves the pressurized injection of a fluid (fracturing fluid) into geologic formations (shale formations or unusually tight rock formations consisting of a clastic sedimentary rock composed of silt to clay sized

grains) until the reservoir rock cracks (causing fractures in the formations) and then extending that fracture by continued injection of fluid. A solid proppant, typically sand, is also injected into the formation with the fracturing fluid so that the fracture cannot close and remains propped open by the proppant left behind when pumps are switched off. This creates a flow path of low resistance for reservoir fluids to be rapidly produced from the reservoir. The illustration is shown in Figure 7.
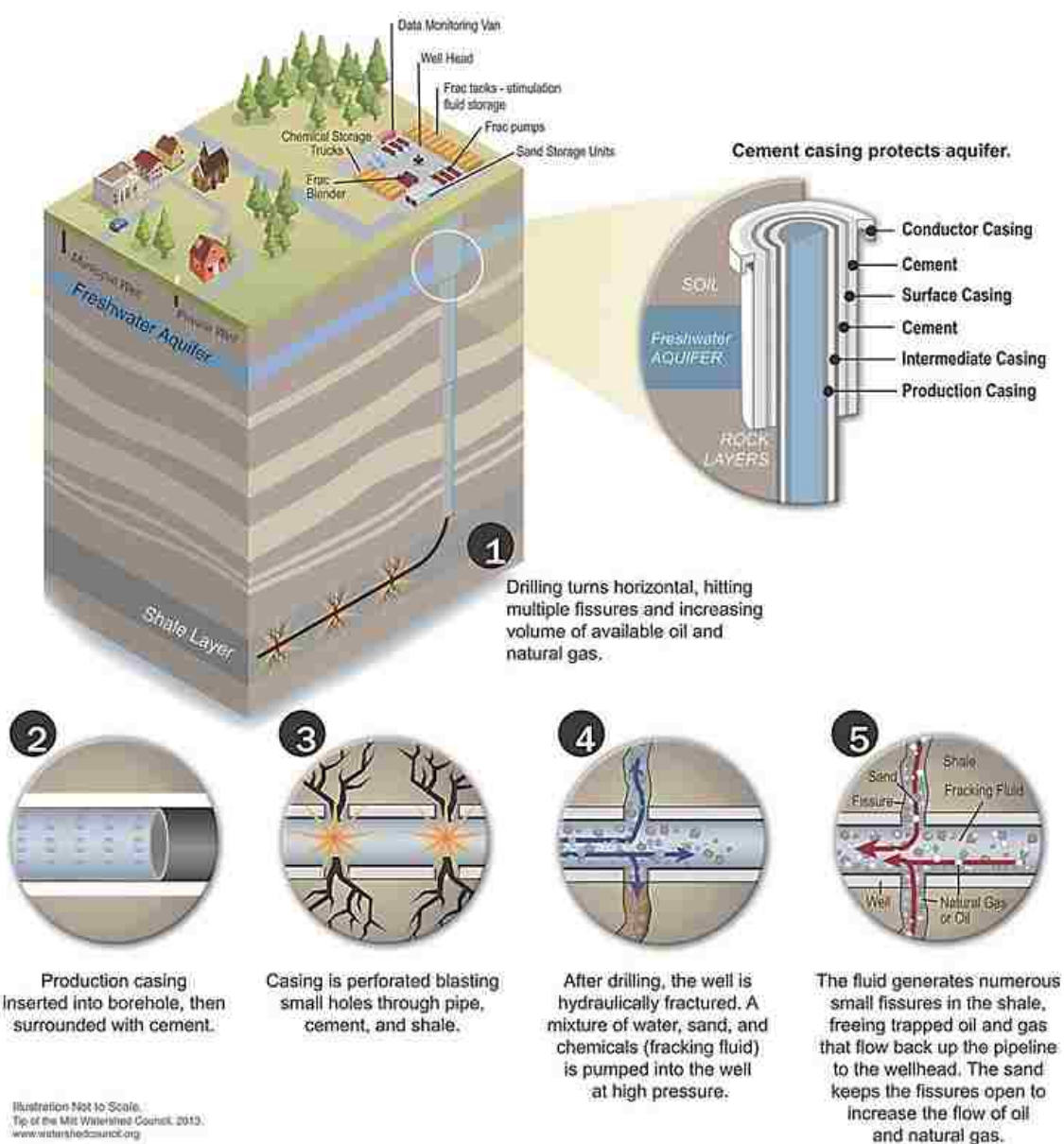
Figure 7: Hydraulic fracturing processes
(Tip of the Mitt Watershed Council, 2013)

The goal of hydraulic fracturing is to create a highly conductive flow path to ease flow from the tight matrix into the wellbore. This technique will allow the flow of fluids and/or gases through the formation to the production well and increase well productivity.

1.5 Research Objectives

LSWF experiments, with and without HF, are proposed in this work to investigate and compare their impacts on ultimate oil recovery in tight carbonate core samples. Moreover, finding the optimum salinity composition and underlying mechanisms during the flooding are side objectives to be completed during the LSWF tests.

1.6 Potential Contributions and Limitations of the Study

Coreflooding tests, with and without simulated induced fracture, were conducted in the laboratory. Results of these experiments potentially may provide support and knowledge to practicing engineers, academician and researchers.

All experiments must have the limitations. This experiment was conducted in small scale at the laboratory, so many factors must be considered to know the results on the bigger scale. Fractures orientation and inlet-outlet brine composition among other factors that should be varied and analyze more in the future research. Hence, further laboratory study, simulation, and piloting are needed to degrade the level of uncertainty.

Chapter 2: Experimental Procedure and Materials

An experimental set up is designed to perform coreflooding tests by sequential brine injection with and without simulated induced single fracture.

2.1 Materials

The including materials for the experiment were provided by Abu Dhabi National Oil Company (ADNOC): crude oil, core samples, and composition of synthetic brine (injected water). Crude oil and core sample were given by ADNOC and the brines were artificially made in the United Arab Emirates University (UAEU) Laboratory.

2.1.1 Crude Oil

Crude oil sample that used in this study is from Asab Field. Asab Field is one of the five major field operated by Abu Dhabi Company for Onshore Petroleum Operation Ltd. (ADCO). This carbonate reservoir with a total proven oil reserve of 3.6 billion barrels was discovered in 1965.

Physical properties of the dead oil are listed in Table 1. Density and API gravity values of the dead oil were measured using both a hydrometer and an Anton Paar digital densitometer at 20 °C.The light asab crude oil was filtered through a 5 mm filter paper prior to any laboratory application. No asphaltene precipitation was observed during the storage. The acid number of crude oil is 0.07 mg KOH/g, measured using the standard titration procedure ASTM D664. Oil viscosity was measured using rolling ball viscometer at 20 °C.

.

Table 1: Physical properties of Asab Crude Oil

Property	Unit	Value
Density at 20° C	API	39.48
Gravity at 20° C	g/cc	0.8276
Viscosity at 20° C & 14.7 psia	mPa.s-cP	2.927
Viscosity at 123° C & 3100 psia (Pres)	mPa.s-cP	1.8593

The chemical analysis of the Asab Crude Oil was analyzed using gas chromatography and reported in Table 2.

Table 2: Chemical analysis of Asab Crude Oil

No.	Substance	Mole Fraction	No.	Substance	Mole Fraction
1	C9	0.50019	17	C23	0.01425
2	C10	0.00022	18	C24	0.01227
3	C11	0.00039	19	C25	0.01062
4	C12	0.03773	20	C26	0.00853
5	C13	0.04466	21	C27	0.00712
6	C14	0.0081	22	C28	0.00554
7	C15	0.09362	23	C29	0.00288
8	C16	0.01655	24	C30	0.00397
9	C17	0.01747	25	C31	0.0033
10	PRISTANE	0.07574	26	C32	0.00284
11	C18	0.01175	27	C33	0.00019
12	PHYTANE	0.07417	28	C34	0.00025
13	C19	0.01318	29	C35	0.00083
14	C20	0.0074	30	C36	0.00053
15	C21	0.01219	31	C37	0.00021
16	C22	0.0133	32	C38	0.00001
Total					1

2.1.2 Brines

Five brines were used in this study. These brines include the formation water of Asab Field (FW), seawater (SW), seawater diluted 10 times (SW/10), seawater

diluted 50 times (SW/50) and seawater with sulfate concentration spiked 6 times (SW $6xSO_4^{-2}$).

FW with Total Dissolved Solids (TDS) of 157,482 mg/L, the density of 1.1034 g/ml and a viscosity of 1.35 cP at ambient conditions. SW sample was collected by Abu Dhabi Oil Company from a location 60 km from Asab field in the Arabian Gulf and an ionic analysis was performed. SW with 62,523 mg/L of TDS was synthetically prepared in the laboratory. SW/10 and SW/50 were then prepared by diluting the SW and SW $6xSO_4^{-2}$ is SW with 6 times increased of sulfate ion (spiking). Dilution and spiking calculations and procedures used for brine preparation are presented in Appendixes A and B.

Brine calculations and synthetic preparation of all the brines were carried out following the procedure presented in Appendix A, after ionically balancing the brine compositions. Tables 3 shows the composition of all brines used in this study.

Density and viscosity of brines were measured using the pycnometer and canon-fenske, respectively, and the results are presented in Table 4.

Table 3: Compositions of the five brines

Ion	FW		SW		SW/10		SW/50		SW 6x SO4	
	TDS (mg/L)	Salinity (ppm)	TDS (mg/L)	Salinity (ppm)	TDS (mg/L)	Salinity (ppm)	TDS (mg/L)	Salinity (ppm)	TDS (mg/L)	Salinity (ppm)
Sodium	44261	44312	19054	19076	1905	1908	381	382	24137	24165
Calcium	13840	13856	690	691	69	69	14	14	690	691
Magnesium	1604	1606	2132	2134	213	213	43	43	2132	2134
Potassium	0	0	672	673	67	67	13	13	672	673
Chloride	96560	96670	35836	35877	3584	3588	717	718	35836	35877
Bicarbonate	332	332	123	123	12	12	2	2	123	123
Sulphate	885	886	3944	3949	394	395	79	79	9254	9265
Total	157482	157662	62451	62523	6245	6252	1249	1250	72844	72928

Table 4: Density and viscosity of the five brines

No.	Brine	Density (g/ml)	Viscosity (cP)
1	FW	1.103	1.35
2	SW	1.034	1.19
3	SW/10	1	1.07
4	SW/50	1	1.03
5	SW 6xSO$_4^{-2}$	1.05	1.26

2.1.3 Core Samples

Nine chalky limestone (CaCO$_3$) core samples from Zakum Oil Field were used for this work. These core samples were selected and prepared for the study (Appendix C illustrates core preparation procedures) such that they share a low initial air permeability (screened using Vinci PoroPerm instrument as described in Appendix D) of less than 1.7 millidarcy that which would be considered as LPCR.

2.2 Experimental Procedure

A flow chart demostrating the sequence of the laboratory tests performed in this study is shown in Figure 8 below.
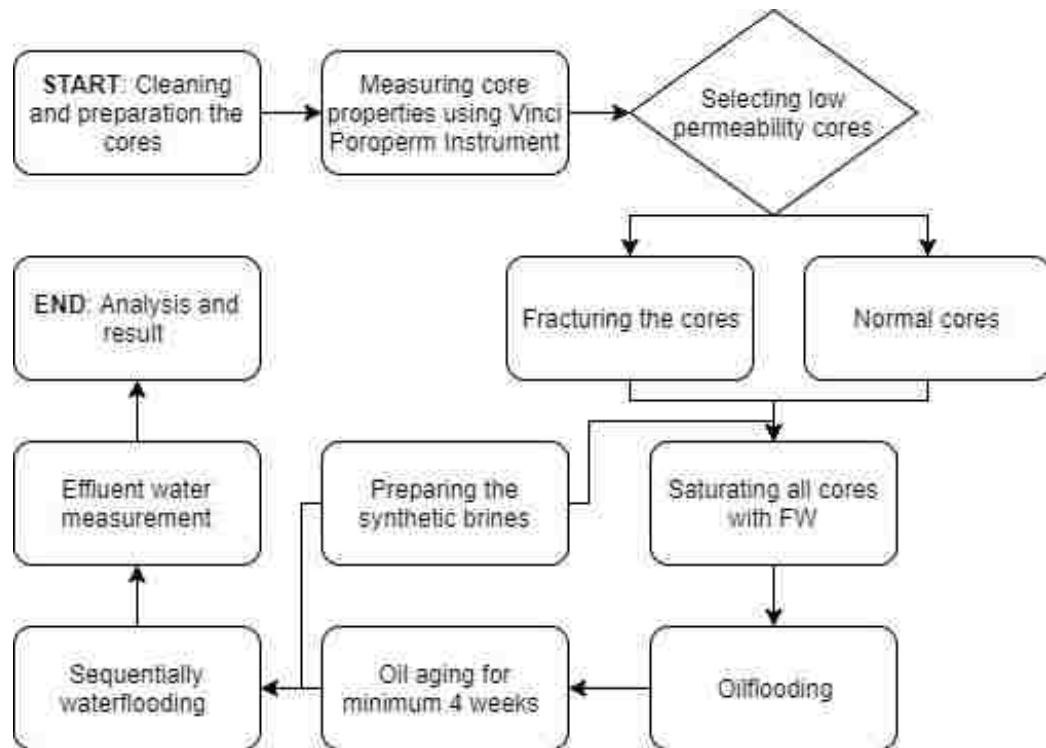
Figure 8: Flowchart illustrating the sequence of laboratory test

2.2.1 Preparing and measuring core properties

Before the experiment started, cleaning the cores was performed to ensure that there is residual fluid and thoroughly dried. A soxhlet extraction apparatus was used for the cleaning followed by drying the cores using the oven, details procedure explained in Appendix C.

Once the cores were dry, measurement of weight and dimension were conducted. Weight measured using digital weight scale, length and diameter measured using a digital caliper and followed by measuring the porosity, grain density and permeability using the nitrogen gas. Measurements were done using Poroperm Instrument (Figure 9). Following steps could be read on Appendix D. Those measurements are essentials for the screening of the samples in order to get low

permeability. Initially, about 18 cores were measured, however only 9 selected tight cores that matched with the criteria required at the next stages, presented in Table 5.

Table 5: Basic cores data

Sample id	Dry wt (gm)	Length (cm)	Diameter (cm)	Pore vol. air (cc)	Bulk vol. (cc)	Grain vol. air (cc)	Grain den. (gm/cc)	Porosity air (%)	Permeability	
									Air (md)	Liquid (md)
ZK-454-2	171.93	6.818	3.801	13.45	77.4	63.94	2.69	17.4	0.15	0.09
ZK-454-3	174.4	6.932	3.803	13.7	78.77	65.07	2.68	17.4	0.25	0.16
ZK-454-4	175.95	7.103	3.794	14.48	80.33	65.85	2.67	18	0.24	0.15
ZK-454-5	169.77	6.998	3.801	15.8	79.44	63.64	2.67	19.9	1.06	0.73
ZK-454-6	135.81	5.418	3.812	10.86	61.86	51	2.66	17.5	0.49	0.32
ZK-454-11	124.35	5.305	3.793	13.95	59.97	46.02	2.7	23.3	0.02	0.01
ZK-454-13	141.22	6.234	3.801	18.43	70.77	52.33	2.7	26	0.98	0.66
ZK-454-20	125.13	5.279	3.806	13.66	60.08	46.43	2.7	22.7	0.05	0.03
ZK-454-27	131.59	5.684	3.8	15.7	64.49	48.79	2.7	24.3	1.7	1.2

Figure 9: Poroperm instrument

2.2.2 Simulating a single induced fracture

The fracture was created parallel to the length of the cores as illustrated in Figure 6. Cutting the core sample into equal halves by along its length. The following

steps of fracturing demonstrated in Figure 10. Complete steps are shown in Appendix C.

Figure 10: Simulating a single induced fracture

The core was slabbed into two equal halves, parallel to length (left), pieces of aluminium foil were placed in between to keep the fractures open (middle), and outer core covered with aluminum foil to keep the core intact (right).

Four core samples were subjected to the above fracture simulating. These core samples are ZK-454-6F, 11F, 20F, and 27F.

2.2.3 Preparation of brines

All synthetic brines were prepared in the laboratory following the ADNOC brines composition guideline. Deionized water was mixed with specified salts by stirrer until the proper composition is reached. Detailed steps are explained in Appendix A.

2.2.4 Water saturating

Core plugs were fully saturated by FW using the core saturation apparatus (Figure 11), with details are explained in Appendix C. Then, FW was injected to the

cores using the coreflooding system (Figure 13) to get the absolute liquid permeability of the cores.

Artificial fracturing could be considered as successful, shown by increasing the absolute liquid permeability presented in Table 6. However, fracturing method should be investigated further for future research since the incremental of core permeabilities are heterogeneous.

Figure 11: Core water saturation apparatus

Table 6: Liquid permeability before and after fracturing

Core no	Permeability liquid(mD)		Folds of permeability increase
	initial	fractured	
ZK-454-6 F	0.32	2.23	7.0
ZK-454-11 F	0.02	6.97	348.3
ZK-454-20 F	0.02	3.02	150.8
ZK-454-27 F	1.7	3.88	2.3

2.2.5 Oilflooding and aging process

All core plugs were then oil flooded (Figure 12) until no more water was produced and then aged for 5 weeks. The procedure of oil flooding is completely explained in Appendix D. Table 7 presents the results of initial water saturation (Swi) and oil saturation (Soi) for all nine core samples used in this work.

Figure 12: Oil flooding

Table 7: Selected cores data

No.	Core ID	Length (cm)	Diameter (cm)	Pore Vol by water (cc)	Porosity by water (%)	Permeability by water (md)	Produced Water (cc)	Swi	Soi
1	ZK-454-2	6.818	3.801	11.818	15.276	0.09	9.5	0.196	0.804
2	ZK-454-3	6.932	3.803	11.628	14.767	0.16	9.1	0.217	0.783
3	ZK-454-4	7.103	3.794	12.244	15.247	0.15	10	0.183	0.817
4	ZK-454-5	6.998	3.801	13.622	17.154	0.73	11.3	0.170	0.830
5	ZK-454-13	6.234	3.801	15.688	22.178	0.66	11.5	0.267	0.733
6	ZK-454-6 F	5.418	3.862	9.075	14.299	2.23	7	0.229	0.771
7	ZK-454-11 F	4.619	3.843	9.888	18.455	6.97	7.2	0.272	0.728
8	ZK-454-20 F	4.703	3.856	9.045	16.469	3.02	7.4	0.182	0.818
9	ZK-454-27 F	5.684	3.850	12.416	18.764	3.88	10	0.195	0.805

2.2.6 Waterflooding

Waterflooding stage is the major part of the study. It was intended to assess selected brines potential in enhancing the oil recovery under reservoir condition. Floodings were conducted sequentially started with high salinity brines and followed by lower salinities and sulfate spiked using the coreflooding system set up (Figure 13). There are 9 coreflooding scenarios, presented in Table 8.

Figure 13: Coreflooding system apparatus

Table 8: Waterflooding scenarios

No.	Sample id	Order of brines injected				
		1st	2nd	3rd	4th	5th
1	ZK-454-2	SW	SW/10	SW/50	SW 6xSO_4^{-2}	
2	ZK-454-3	FW	SW	SW/10	SW/50	SW 6xSO_4^{-2}
3	ZK-454-4	SW/10	SW/50	SW 6xSO_4^{-2}		
4	ZK-454-5	SW/50	SW 6xSO_4^{-2}			
5	ZK-454-13	SW 6xSO_4^{-2}	SW/50			
6	ZK-454-6 F	FW	SW	SW/10	SW/50	SW 6xSO_4^{-2}
7	ZK-454-11 F	SW/10	SW/50	SW 6xSO_4^{-2}		
8	ZK-454-20 F	SW	SW/10	SW/50	SW 6xSO_4^{-2}	
9	ZK-454-27 F	SW 6xSO_4^{-2}	SW/50			

All the tests were conducted under similar reservoir conditions, an overburden pressure of 2500 psia (applied using the hydraulic pump) and temperature increased to 90ºC (core holder is equipped with a heating jacket). The injection rate of brines was constant at 1 cc/min, through-out each flooding scenario. A back pressure regulator was installed to control the outlet pressure at 100 psi to regulate the flow and avoid extra pressure build-up after heating the system. The detailed procedures of core flooding experiments are presented in Appendix E.

2.2.7 Examination of effluent water

Four of effluent water properties were analyzed, namely, salinity, resistivity, pH, and conductivity. Salinity in ppm and resistivity in ohm.meter were measured by using a digital resistivity meter (Figure 14).

Figure 14: Digital resistivity meter

Conductivity (mS/cm) and pH were measured by using digital conductivity meter and digital pH meter illustrated in Figure 15. Detailed steps of measurement are illustrated in Appendix F.

Figure 15: Digital conductivity meter

Chapter 3: Results and Discussions

The ultimate objective of the research is to evaluate the performance of high and low salinity water flooding of fractured and non-fractured low permeability oil reservoirs. The results will shed some light on the way to proceed forward with a possible recovery technique for low permeability oil reservoirs.

During the waterflooding experiment, produced and injected fluids and pressure drop across the cores were measured carefully as a function of time. Table 9 shows an example of complete collected and calculated results of a coreflooding from core ZK-454-3. Rest of tables for each core could be seen in Appendix G. Results generally presented in the graphical form of recovery factor RF as a function of pore volume injected as illustrated in Figure 16 and presented in Table 9.

Table 9: Recovery Factor of ZK-454-3

No.	Injected Brines	Voil Produced (cc)	Vwater Produced (cc)	Incremental RF (%)	RF (%)	Incremental PV injected	PV injected
1	FW	0	0	0.000	0.000	0.000	0.000
		3.9	6.1	42.857	42.857	0.860	0.860
		0.8	9.2	8.791	51.648	0.860	1.720
		0.4	9.6	4.396	56.044	0.860	2.580
		0.2	9.8	2.198	58.242	0.860	3.440
		0.1	9.9	1.099	59.341	0.860	4.300
		0	9.4	0.000	59.341	0.808	5.108
		0	0	0.000	59.341	0.000	5.108
2	SW	0.6	17.33	6.593	65.934	1.542	6.651
		0	34.67	0.000	65.934	2.981	9.632
		0	0.00	0.000	65.934	0.000	9.632
3	SW/10	0.3	17.43	3.297	69.231	1.525	11.157
		0	34.87	0.000	69.231	2.999	14.156
		0	0.00	0.000	69.231	0.000	14.156
4	SW/50	0.2	17.37	2.198	71.429	1.511	15.667
		0	34.73	0.000	71.429	2.987	18.654
		0	0.00	0.000	71.429	0.000	18.654
5	SW 6xSO_4^{-2}	0.1	17.45	1.099	72.527	1.509	20.163
		0	34.90	0.000	72.527	3.001	23.164

Moreover, injection pressure values during the test were taken periodically. Pressure difference (Δ Pressure) is differential pressure, dP, between injection pressure and backpressure valve (100 psia). An example of data shown in Table 10. ΔP's were plotted as a secondary y-axis in the graph as shown in Figure 16.

Table 10: Pressure differential of ZK-454-3

Injected Brines	No.	Vwater Injected (cc)	Cummulative Vwater Injected (cc)	PV injected	Δ Pressure (psi)
FW	1	0.000	0.000	0.000	0
	2	8.486	8.486	0.730	1143
	3	8.486	16.971	1.460	1320
	4	8.486	25.457	2.189	1319
	5	8.486	33.943	2.919	1307
	6	8.486	42.429	3.649	1257
	7	8.486	50.914	4.379	1224
	8	8.486	59.400	5.108	1200
SW	1	7.514	66.914	5.755	1145
	2	7.514	74.429	6.401	1125
	3	7.514	81.943	7.047	1078
	4	7.514	89.457	7.693	1009
	5	7.514	96.971	8.340	955
	6	7.514	104.486	8.986	944
	7	7.514	112.000	9.632	930
SW/10	1	8.767	120.767	10.386	900
	2	8.767	129.533	11.140	873
	3	8.767	138.300	11.894	865
	4	8.767	147.067	12.648	850
	5	8.767	155.833	13.402	852
	6	8.767	164.600	14.156	851
SW/50	1	8.717	173.317	14.905	840
	2	8.717	182.033	15.655	830
	3	8.717	190.750	16.405	830
	4	8.717	199.467	17.154	814
	5	8.717	208.183	17.904	820
	6	8.717	216.900	18.654	818
SW 6xSO$_4^{2-}$	1	10.490	227.390	19.556	840
	2	10.490	237.880	20.458	824
	3	10.490	248.370	21.360	820
	4	10.490	258.860	22.262	810
	5	10.490	269.350	23.164	811
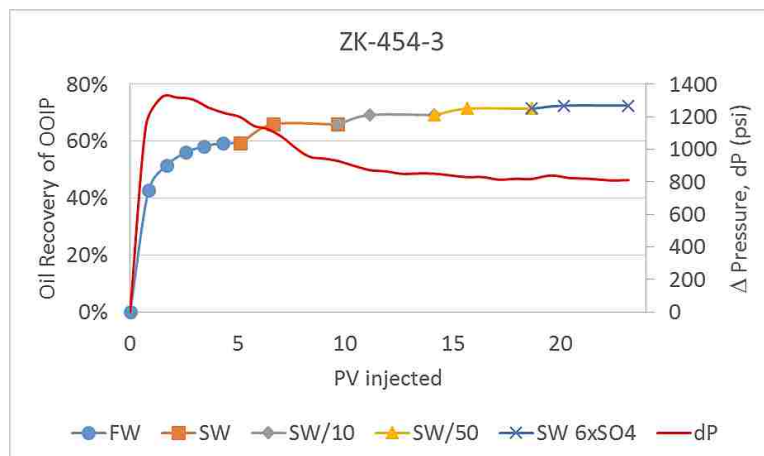
Figure 16: Oil recovery and ΔP by the function of PV injected for ZK-454-3 sample

In addition to, the Effective permeability of water (Kw_{eff}) were calculated using Darcy's Law equation at residual oil residual (Sor), when there is no oil produced anymore, during every stage of waterflooding. Water viscosity at 90°C was estimated roughly using a function of salinity, temperature, and viscosity of seawater (El-dessouky, 2002). The viscosity results are presented in Table 11 and a comparison of endpoint water permeability for different runs is shown in Figure 17.

Table 11: Estimated brine viscosity at 90°C

No.	Brine	Viscosity at 90° C
1	FW	0.48
2	SW	0.37
3	SW/10	0.32
4	SW/50	0.31
5	SW 6xSO_4^{-2}	0.38
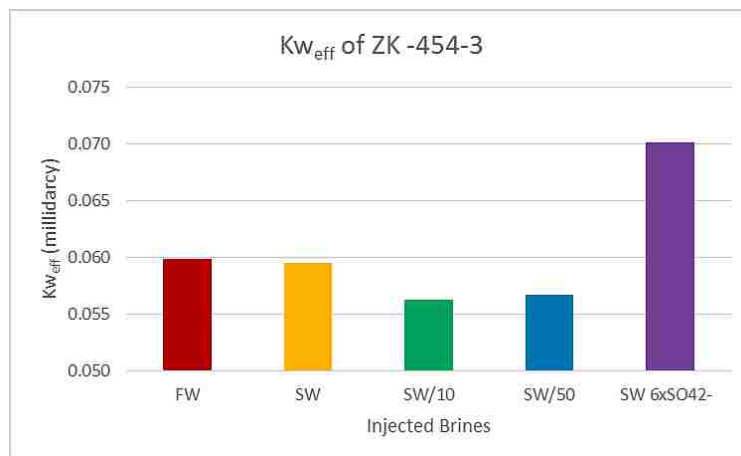
Figure 17: Endpoint water permeability for different waters of ZK-454-3

3.1 Low Salinity Waterflooding of Non-Fractured Cores

The results of coreflooding for normal cores are shown in Table 12 below. The following five different water were employed using different consequential: FW, SW, SW/10, SW/50, SW 6xSO$_4^{-2}$. The sequentially waterflooding test started with SW/10 produces the most oil recovery with 76% of OOIP which required 13.803 PV of water injection, followed by the test that started by SW/50, FW, SW, and SW 6xSO$_4^{-2}$. However, by decreasing the salinity is proven for not only enhancing the oil recovery but also reducing the volume of water needs to be injected. As shown, sequential of cores ZK-454-2 and ZK-454-3 have produced almost the same oil recovery. On the other hand, it required more pore volume of water to recover the same amount of oil in case of sequential ZK-454-3 (23 PV) compared to sequential ZK-454-2 (18 PV). It is most likely starting the sequential with formation brine results in additional water required for low salinity water to contact the oil and change the system wettability. Water shielding phenomenon is taken place in this case.

Table 12: Brief waterflooding result of normal cores

Core ID	Injected Brines	Voil Produced (cc)	PV Injected (cc)	Vwater Injected (cc)	Incremental RF (%)	RF (%)	Incremental PV injected	PV injected	ΔP at S_{or} (psi)	Kw_{eff} at Sor estimated (millidarcy)
ZK-454-2	SW	6.1	53	59.1	64.211	64.211	5.001	5.001	1250	0.044
	SW/10	0.3	52.3	52.6	3.158	67.368	4.451	9.452	1136	0.041
	SW/50	0.25	52.1	52.35	2.632	70.000	4.430	13.881	1115	0.041
	SW 6xSO$_4^{-2}$	0.15	52.4	52.55	1.579	71.579	4.447	18.328	1120	0.050
ZK-454-3	FW	5.4	54	59.4	59.341	59.341	5.108	5.108	1200	0.060
	SW	0.6	52	52.6	6.593	65.934	4.524	9.632	930	0.060
	SW/10	0.3	52.3	52.6	3.297	69.231	4.524	14.156	851	0.056
	SW/50	0.2	52.1	52.3	2.198	71.429	4.498	18.654	818	0.057
	SW 6xSO$_4^{-2}$	0.1	52.35	52.45	1.099	72.527	4.511	23.164	811	0.070
ZK-454-4	SW/10	7.2	56.8	64	72.000	72.000	5.227	5.227	1105	0.045
	SW/50	0.3	52.2	52.5	3.000	75.000	4.288	9.515	811	0.059
	SW 6xSO$_4^{-2}$	0.1	52.4	52.5	1.000	76.000	4.288	13.803	788	0.074
ZK-454-5	SW/50	8.1	55	63.1	71.681	71.681	4.632	4.632	381	0.123
	SW 6xSO$_4^{-2}$	0.2	52.5	52.7	1.770	73.451	3.869	8.501	320	0.180
ZK-454-13	SW 6xSO$_4^{-2}$	7.4	55.6	63	64.348	64.348	4.016	4.016	513	0.100
	SW/50	0.45	52.15	52.6	3.913	68.261	3.353	7.369	415	0.101

Figures 18-21 present oil recovery and pressure drop as a function of pore volume injected for different consequential floodings. All tests were conducted at a constant injection rate of 1 cc/min. A decline in pressure drop was observed in all runs as shown in the Figures 18-21. Generally, declining of the pressure is associated with changing the injection water from high salinity to the lower salinity system. The magnitude of decreasing pressure for each core are identified and the values vary and no pattern was observed. The previous phenomenon was not observed in the case of SW 6xSO$_4^{-2}$ injection mode. No significant declining in the pressure drop was observed in the pressure maintained the same level in most of the cases.
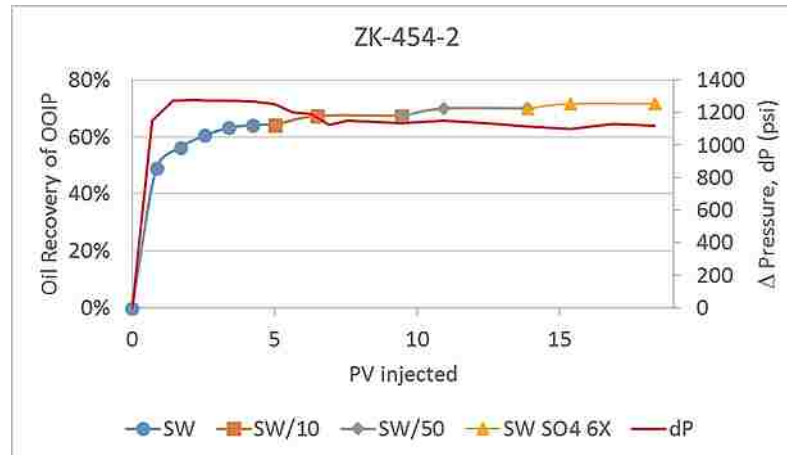
Figure 18: Oil recovery and ΔP by the function of PV injected for ZK-454-2 sample
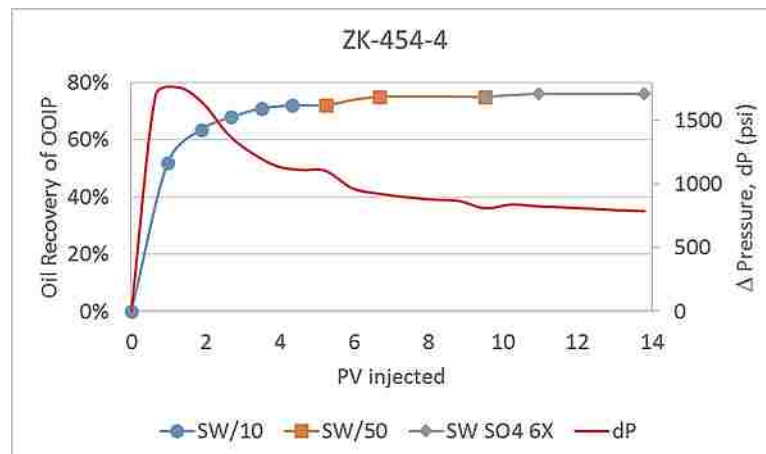
Figure 19: Oil recovery and ΔP by the function of PV injected for ZK-454-4 sample
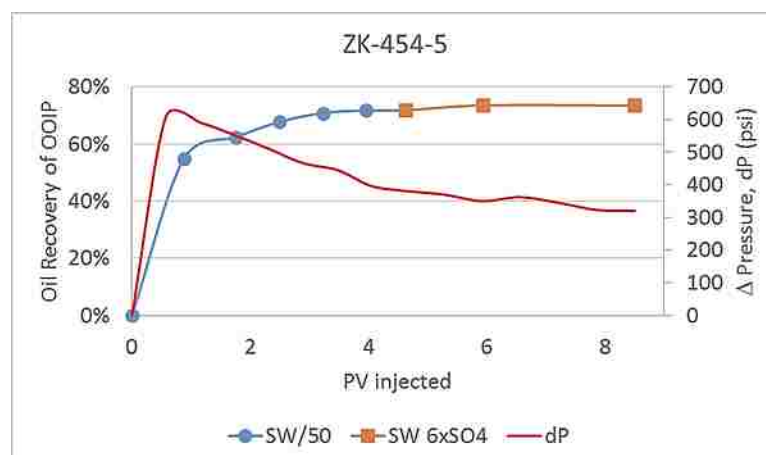
Figure 20: Oil recovery and ΔP by the function of PV injected for ZK-454-5 sample

Figure 21: Oil recovery and ΔP by the function of PV injected for ZK-454-13 sample

Figures 16 and 18-21 show plots of oil recovery and pressure drops as a function of pore volume injection for different consequential runs. Generally, the pressure drop across the cores is declining with increasing pore volume injected. This indicates that permeability is improving as result of mineral dissolution which leads to exposing new surface i.e., wettability alteration. The highest % of pressure drop occurred during sequential 3 and 4 which is 32% and 29% although sequential 3 consists of 5 different brines while sequential 4 consists of 3 different brines starting with SW/10, see Table 12. Results indicate that flooding SW/10 i.e., reducing seawater salinity to around 5000 ppm is the optimum single flood system. A 73% of the original oil in place was recovered by SW/10 compared to 59.4% OOIP recovered by formation brine. Sequential no. 4 which consists of SW/10 followed by SW/50 and SW $6xSO_4^{-2}$ is the optimum sequential system which recovered 76% OOIP. This indicates that addition of two brine SW/50 and SW $6xSO_4^{-2}$ improve the oil recovery by 3% OOIP.

Figure 22 presents a comparison of the endpoint water relative permeability for different waters employed in this study. The results clearly support the conclusion that wettability is the dominant mechanism and the system is moving toward more water

wet as the lowest water relative permeability associated with optimum salinity system of SW/10. The decline of the endpoint water relative permeability indicates a shift toward more water wetness (Anderson, 1987).

Figure 22: Endpoint water permeability for different waters of ZK-454-2

Figure 23: Endpoint water permeability for different waters of ZK-454-4

Figure 24: Endpoint water permeability for different waters of ZK-454-5

Figure 25: Endpoint water permeability for different waters of ZK-454-13

Figures 23-25 display end point water relative permeability for sequential's 4, 5, and 13. Again, most of the results confirm the conclusion of an association between reduction of endpoint water relative permeability and improvement of oil recovery as a result of the shift of the wettability of the system to more water wetness. Consequential 13 does not display the same trend because the starting brine is SW $6xSO_4^{-2}$ which has an insignificant effect on the system wettability and that results in low recovery efficiency.

Figure 26 presents flow resistance factor as a function of pore volume injection. Flow resistance factor defined as a ratio of pressure drop Δp across the core over maximum pressure drop across Δp$_{max}$ the core. Results indicate that sequential 4 exhibits the least flow resistance which again confirms the previous conclusion.
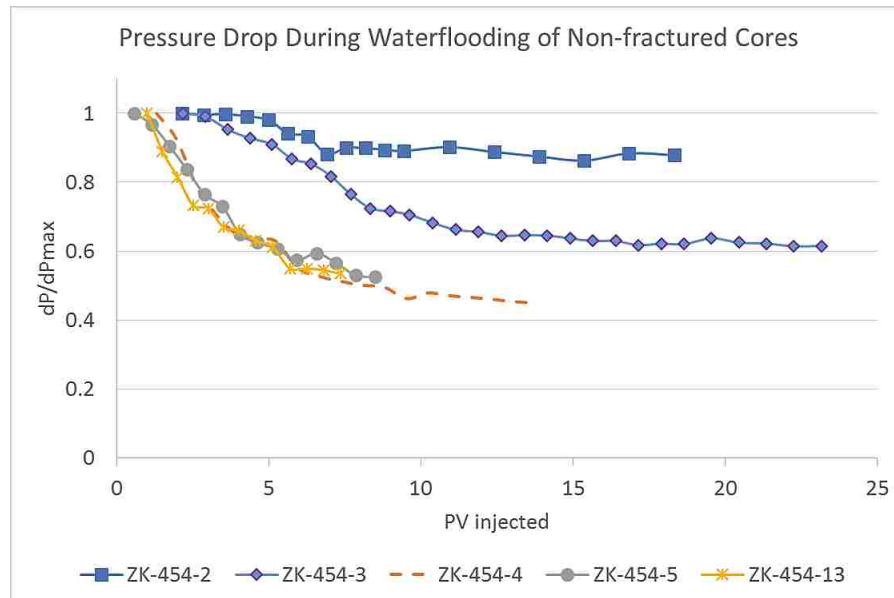
Figure 26: Flow resistance factor versus pore volume injected, non-fracture system

3.2 Low Salinity Waterflooding of Fractured Cores

Many operators believe that fracturing the oil reservoir is the only way to recover oil from low permeability oil reservoirs. In this section, evaluation of the performance of the fractured system and compare the results to the non-fractured system. The objective is to optimize oil recovery for low permeability oil reservoir through testing the following schemes: high salinity flooding, low salinity flooding, fracture the reservoir and conduct high salinity flooding, fracturing the reservoir and conduct low salinity flooding. Summary of the results of waterflooding for 4 fractured

cores is presented in Table 13. Four sequential brine flooding (6F, 11F, 20F, and 27F) of the fractured cores were conducted at reservoir conditions.

Reservoir fracturing has a significant effect on the performance of brine flooding. Formation brine flooding of the fractured and non-fractured system yields 65.7% and 59.3% of OOIP respectively. Low salinity SW/10 flooding is more effective as compared with high salinity fractured system flooding. Combination of low salinity and fracturing is the ideal oil recovery scheme. A 5% additional oil recovery could be obtained by using the SW/10 brine in fracturing system over the non-fractured system. The optimum sequential system for a fractured system is sequential 11F (SW/10, SW/50, SW $6xSO_4^{-2}$). Sequential 11F produced 82.639% OOIP. Fractured and non-fractured system have the same optimum brine flooding of SW/10.

The pressure drop across the fractured cores exhibits a similar behavior as observed in the case of a non-fractured system which declining with pore volume injected see Figures 27-30. Therefore, it can be concluded that dissolution associated with low salinity flooding which results in an improvement in the system permeability is the mechanism responsible for the improvement of oil recovery.

Table 13: Brief waterflooding result of fractured cores

Core ID	Injected Brines	Voil Produced (cc)	PV Injected (cc)	Vwater Injected (cc)	Incremental RF (%)	RF (%)	Incremental PV injected	PV injected	ΔP at S_{or} (psi)	Kw_{eff} at Sor estimated (millidarcy)
ZK-454-6F	FW	4.6	56.3	60.9	65.714	65.714	6.711	6.711	413	0.135
	SW	0.45	51.4	51.85	6.429	72.143	5.713	12.424	320	0.135
	SW/10	0.25	52	52.25	3.571	75.714	5.757	18.181	280	0.133
	SW/50	0.15	51.2	51.35	2.143	77.857	5.658	23.840	260	0.139
	SW 6xSO_4^{-2}	0.1	52	52.1	1.429	79.286	5.741	29.580	285	0.155
ZK-454-11F	SW/10	5.55	55.2	60.75	77.083	77.083	6.144	6.144	289	0.111
	SW/50	0.25	51.5	51.75	3.472	80.556	5.234	11.378	197	0.158
	SW 6xSO_4^{-2}	0.15	51.9	52.05	2.083	82.639	5.264	16.642	219	0.174
ZK-454-20F	SW	5.3	53.3	58.6	71.622	71.622	6.479	6.479	313	0.120
	SW/10	0.3	52.3	52.6	4.054	75.676	5.815	12.294	308	0.105
	SW/50	0.1	51.9	52	1.351	77.027	5.749	18.043	296	0.106
	SW 6xSO_4^{-2}	0.1	51	51.1	1.351	78.378	5.650	23.693	293	0.131
ZK-454-27F	SW 6xSO_4^{-2}	6.75	50.1	56.85	67.500	67.500	4.579	4.579	299	0.156
	SW/50	0.4	52.3	52.7	4.000	71.500	4.244	8.823	228	0.167
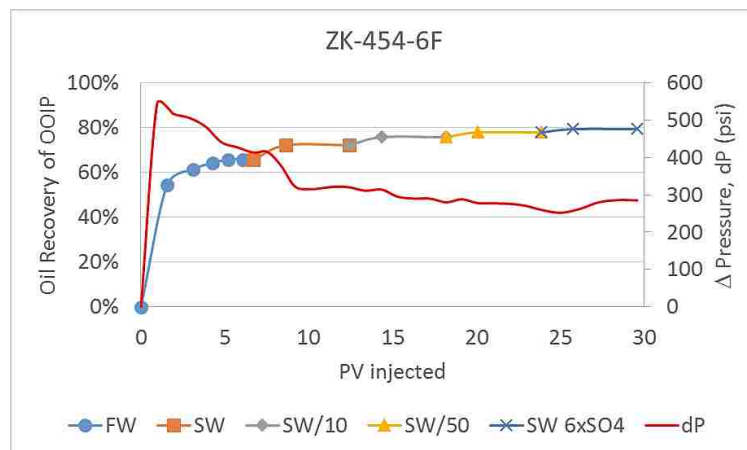
Figure 27: Oil recovery and ΔP by the function of PV injected for ZK-454-6F sample
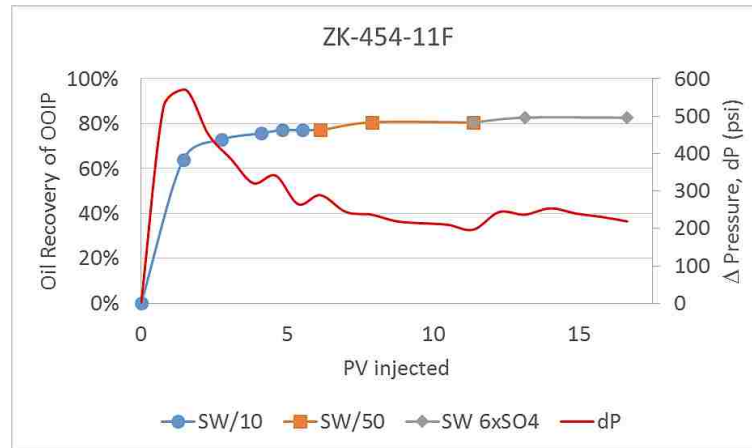
Figure 28: Oil recovery and ΔP by the function of PV injected for ZK-454-11F sample
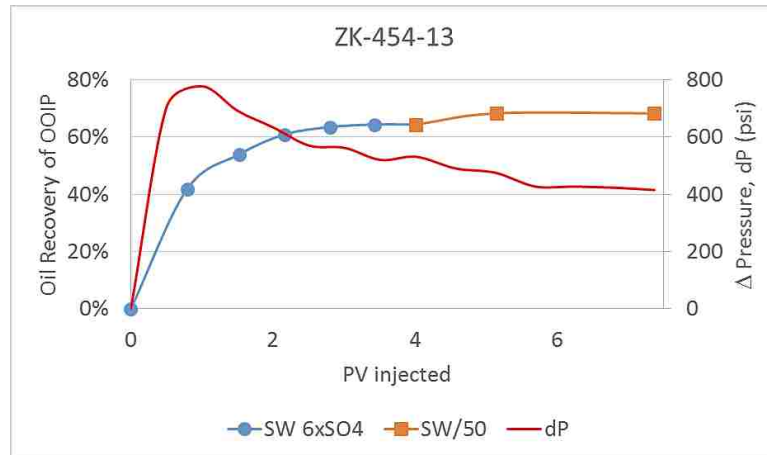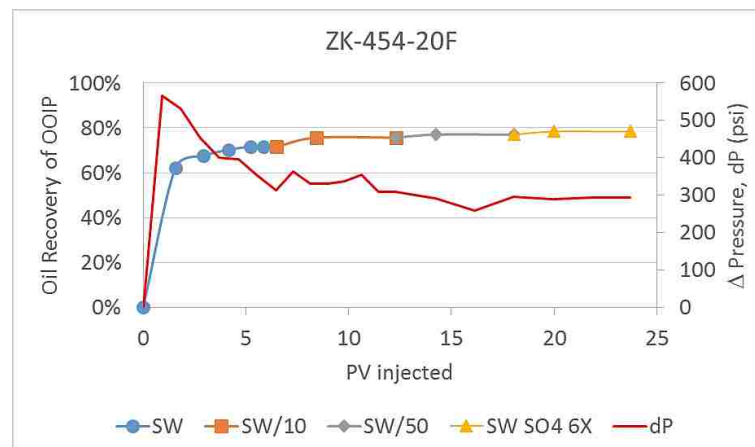

Figure 29: Oil recovery and ΔP by the function of PV injected for ZK-454-20F sample
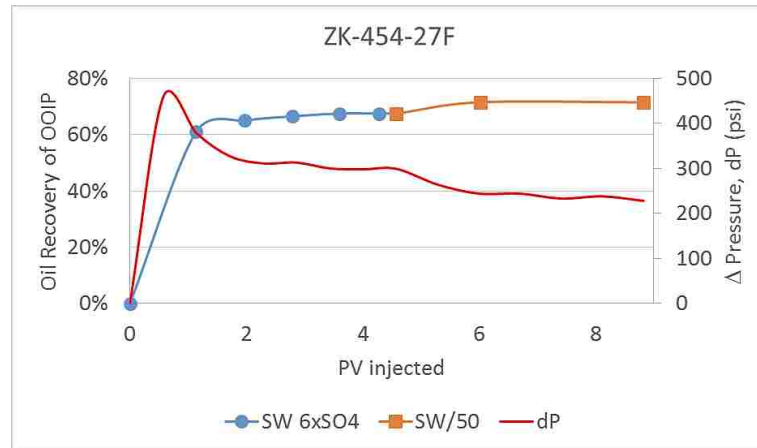
Figure 30: Oil recovery and ΔP by the function of PV injected for ZK-454-27F sample

Figures 31-34 present the comparison of the endpoint water relative permeability for different waters employed in the study of the fractured system. The results are matching a non-fracturing system and clearly supports the conclusion that wettability is the dominant mechanism and the system is moving toward more water wet as the lowest water relative permeability associated with optimum salinity system of SW/10.
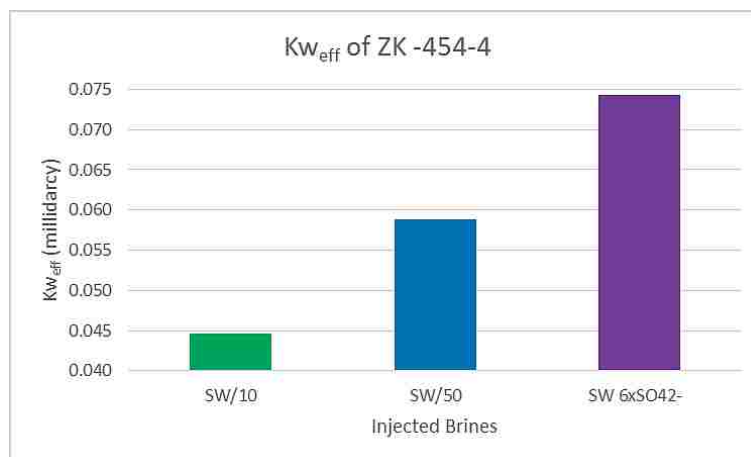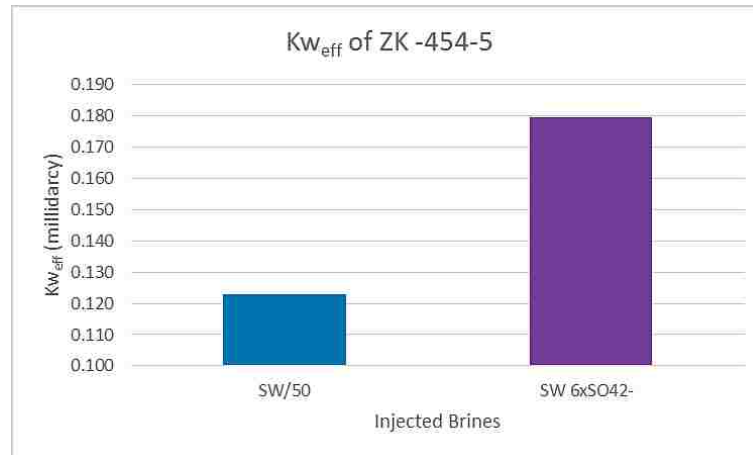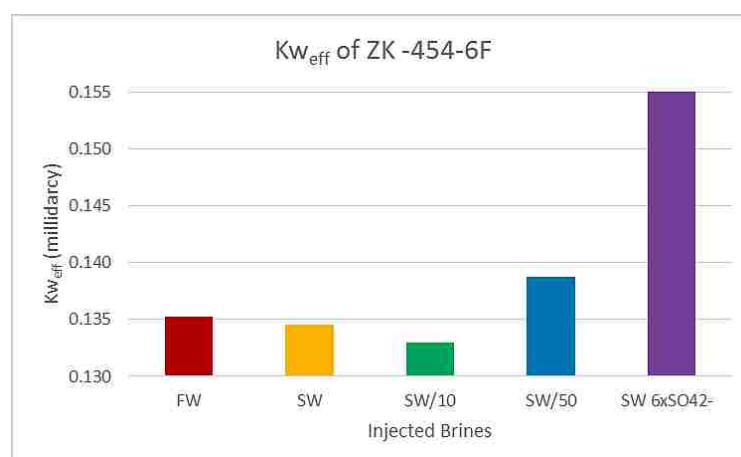

Figure 31: Endpoint water permeability for different waters of ZK-454-6F
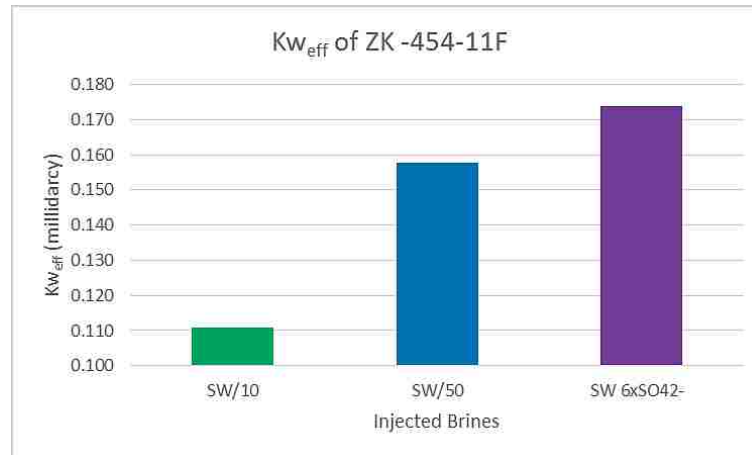
Figure 32: Endpoint water permeability for different waters of ZK-454-11F
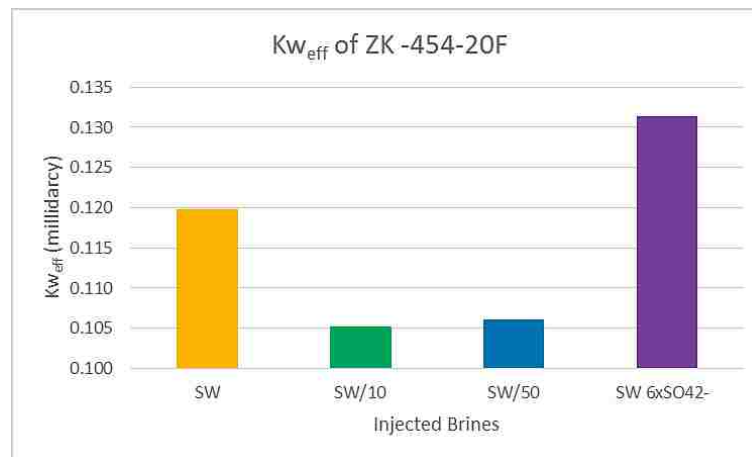
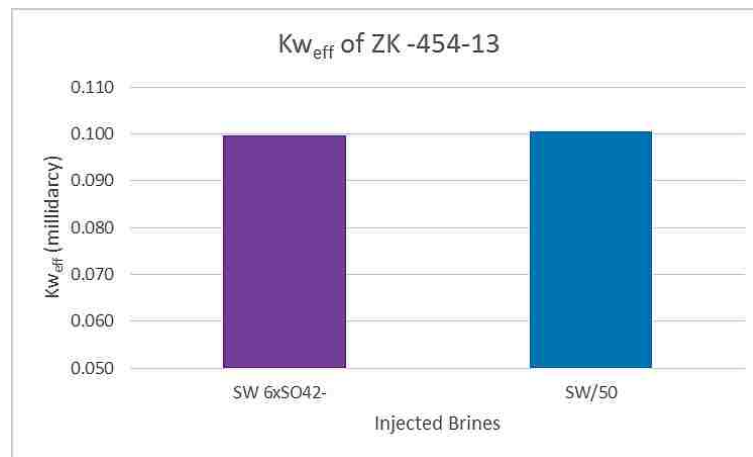Figure 33: Endpoint water permeability for different waters of ZK-454-20F
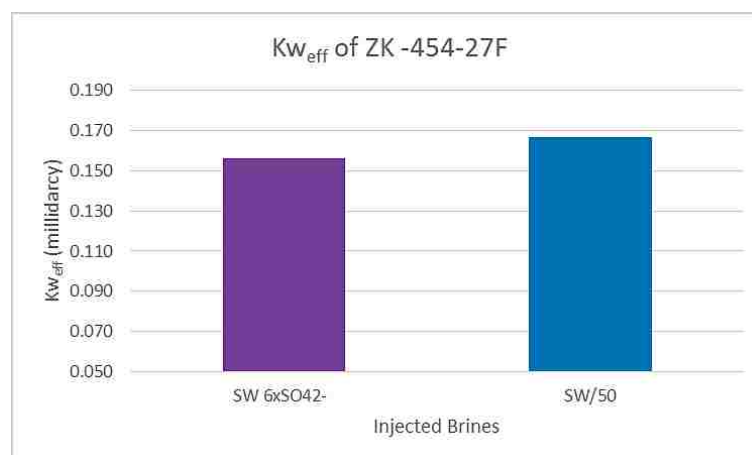
Figure 34: Endpoint water permeability for different waters of ZK-454-27F

Figures 32-34 display end point water relative permeability for sequentials 11F, 20F, and 27F. Most of the results confirm the conclusion of an association between reduction of endpoint water relative permeability and improvement of oil recovery as a result of shift of the wettability of the system to more water wetness. Consequential 27F does not display the same trend because the starting brine is SW $6xSO_4^{-2}$ which has an insignificant effect on the system wettability and that results in low recovery efficiency.

Figure 35 presents flow resistance factor for the fractured system as a function of pore volume injection. Flow resistance factor defined as a ratio of pressure drop Δp across the core over maximum pressure drop across Δp_{max} the core. Results indicate that sequential 11F exhibits the least flow resistance which confirms the previous conclusion of the flood should be initiated with low salinity system of SW/10 i.e., 6252 ppm salinity.
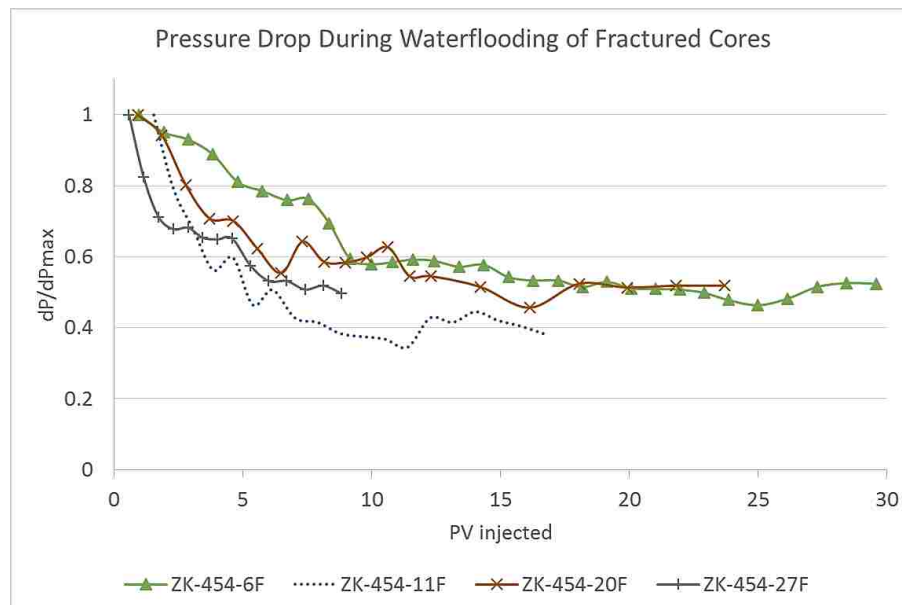
Figure 35: Flow resistance factor versus pore volume injected, fractured systems

3.3 Effluent Water Measurement

Injected brine properties (salinity, resistivity, conductivity, and pH) before and after flooding had been measured in the lab and presented in Table 14. Total Dissolved Solids (TDS) of effluent water were calculated using a proven software TDS converter developed by Chemiasoft, by converting the conductivity to TDS. To ease the analysis results presented in the graphical form below as shown in Figures 36-40.

Results indicate that a maximum dissolution is taken place during SW/10 flooding where TDS increased by 295%. This confirms the findings that dissolution is taken place and that resulted in exposing new surface which leads to alteration of the system wettability. Keeping in mind that SW/10 flooding as a single flood and as starting brine in sequential flood is the optimum flooding system for both fractured and no-fractured system. Evaluation of water salinity prior and post-flooding for all studied systems indicted that SW/10 flooding displayed the highest increase in brine salinity. Post flooding salinity during SW/10 flooding is increased by 229% over prior flooding salinity. This result is in line with the conclusion and that supports the finding. Alteration of salinity and TDS in water after injection is most likely due to fines migration and dissolution during the flooding. Those factors are the main reason for the observed increase in the oil recovery during the LSWF SW/10 as explained by Zahid et al. (2012). Fines migration and dissolution open more path to flow of water and push the oil together with dissolving the limestone which may alter the wettability toward more water wet behavior.

As salinity of effluent water increased, the resistivity will be decreased and conductivity increased as indicated in Table 14. Measurements of the pH in fact that there is a correlation between these 3 factors. No significant alteration of the pH of the

water in the case of SW/10 flooding. Other systems indicated a decrease in the pH of

the effluent except for SW/50 which displayed and increase the pH. Therefore no clear

conclusion can be drawn based on the presented results.

Table 14: Effluent water properties

Injected Water	Salinity (ppm)		Resistivity (ohm*meter)		Conductivity (mS/cm)		pH		TDS (mg/L)	
	Before	After	Before	After	Before	After	Before	After	Before	After
FW	157662	117314	0.068	0.071	197.2	189.5	7.12	6.98	157482	123322
SW	62522	69259	0.136	0.104	89.9	125.3	7.22	6.89	62451	83779
SW/10	6252	20584	1	0.291	11.63	40	7.17	7.18	6245	24673
SW/50	1250	4496	3.53	1.21	3.13	9.47	7	7.33	1249	5446
SW 6xSO_4^{2-}	72927	56565	0.133	0.174	90	71	7.35	7.23	72844	59194
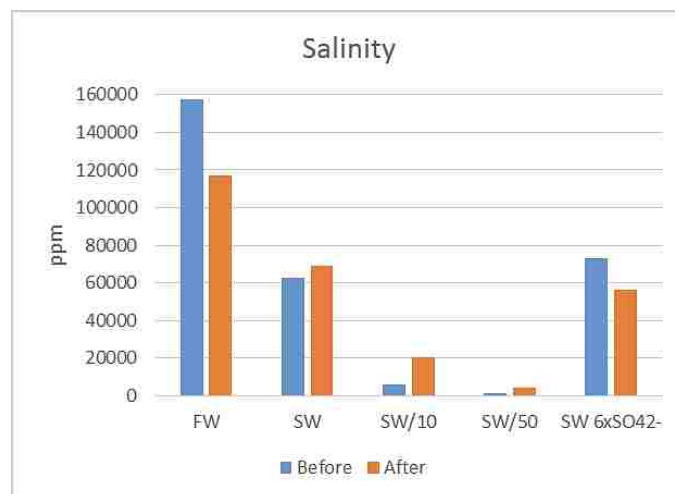
Figure 36: Salinity of brines before and after flooding
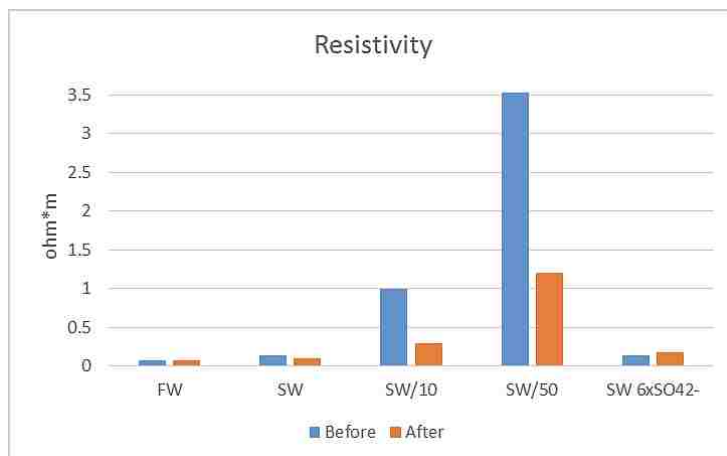
Figure 37: Resistivity of brines before and after flooding
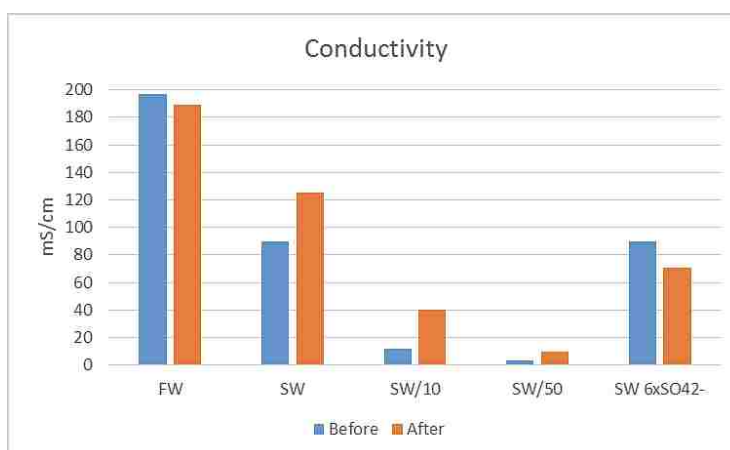
Figure 38: Conductivity of brines before and after flooding

Figure 39: PH of brines before and after flooding
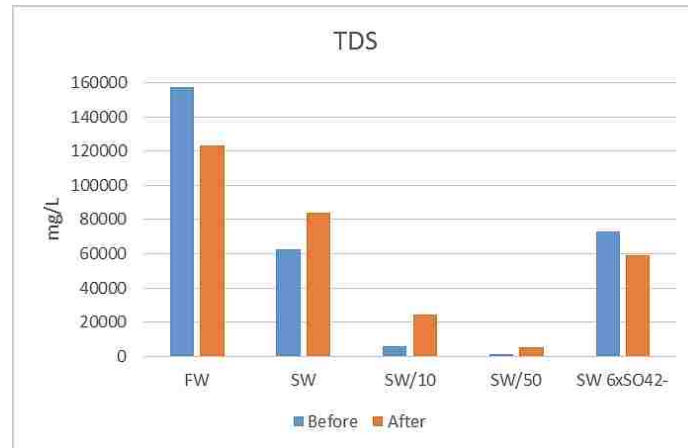
Figure 40: TDS of brines before and after flooding

3.4 Analysis and Comparisons

Secondary recovery stage (the stage when the first brine injected), seawater diluted 10 times is the most prominent brine for the candidate low permeability oil reservoir in both fractured (Figure 42) and nonfractured system (Figure 41) by showing 77% and 72% improvement of oil recovery, respectively. While FW flooding displayed the lowest RF.
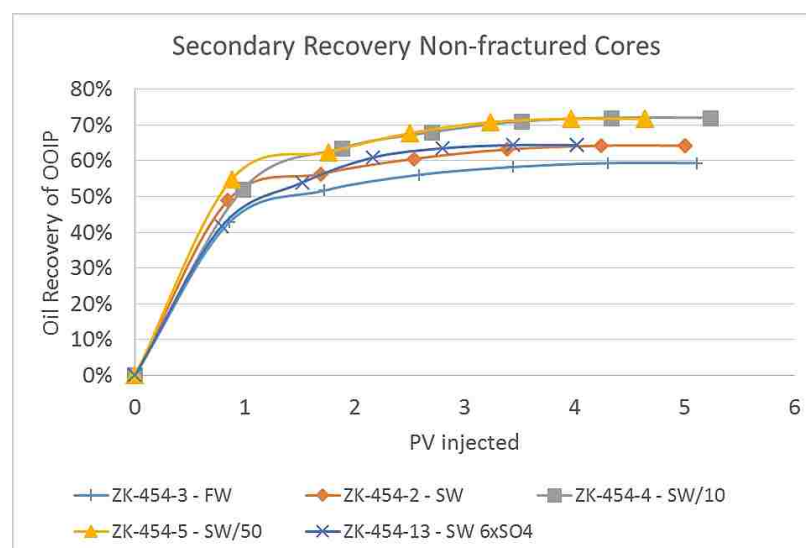
Figure 41: Secondary recovery of non-fractured cores
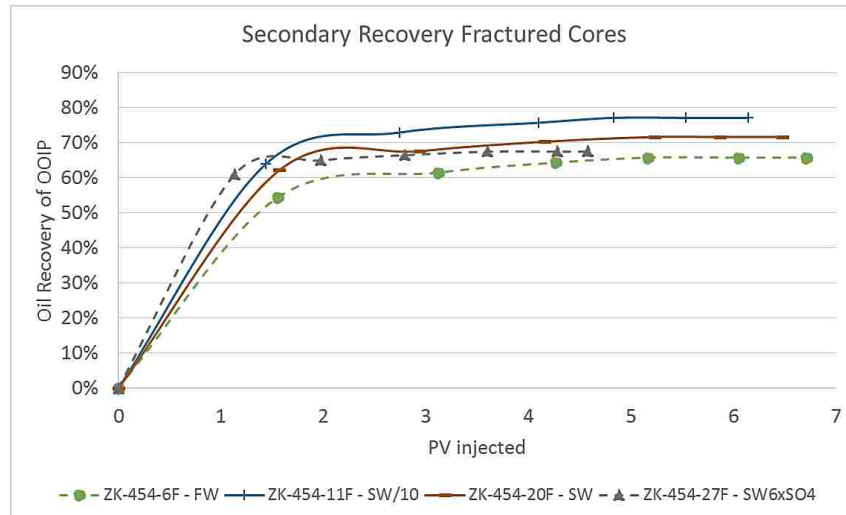
Figure 42: Secondary recovery of fractured cores

In general, decreasing injection water salinity have a significant effect on the flood performance at the secondary flooding stage for both fractured and non-fractured system as presented Tables 15 and 16. The optimum system is SW/10 which produced 12.7% and 11.4% more than base condition (FW injection) for normal and fractured core respectively (Table 15 and 16).

Table 15: Oil recovery improvement value at the secondary recovery of the normal core

Starting water	RF's incremental LSWF (%)
FW	Base
SW	4.870
SW/10	12.659
SW/50	12.341
SW 6xSO_4^{-2}	5.007

Table 16: Oil recovery improvement value at the secondary recovery of the fractured core

Starting water	RF's incremental LSWF (%)
FW	Base
SW	5.907
SW/10	11.369
SW 6xSO$_4$$^{-2}$	1.786

Fracturing the system as expected will result in improvement of oil recovery for both low and high salinity flooding as presented in Table 17. The improvement of oil recovery due to fracturing is mainly due to the improvement of the system permeability and contact area for the injected fluid.

Table 17: Fracturing effects on every stage of flooding

Starting water	RF's incremental differences between fractured and non fractured (%)				
FW	6.374	-0.165	0.275	-0.055	0.330
SW	7.411	0.896	-1.280	-0.228	
SW/10	5.083	0.472	1.083		
SW 6xSO$_4$$^{-2}$	3.152	0.087			

Figure 43 presents a comparison of oil recovery for secondary flood as a function of pore volume injected between fractured and non-fractured systems. Flooding results indicated that salinity optimization has a significant effect on the performance of the flood. Combination of low salinity SW/10 and fracturing (LSF) technically is the recommended scheme of flooding. LSF improves oil recovery over HS by more than 20% OOIP as shown in Figure 43.
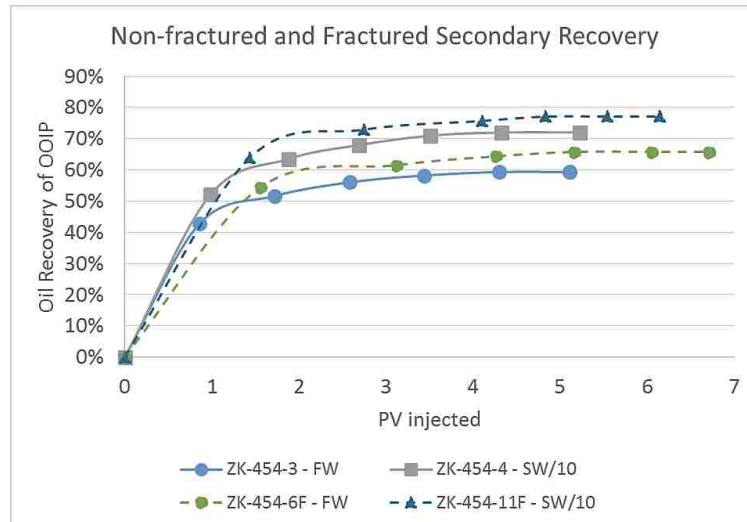
Figure 43: Secondary recovery comparison between fractured and non-fractured cores

Secondary brine flooding endpoint water relative permeability (Krw $_{@S_{or}}$) pattern for both non-fractured and fractured systems are displayed in Figure 44 and 45. The most reduction in the Krw $@S_{or}$ was observed during SW/10 flooding for both systems. A 33% reduction of endpoint relative permeability was estimated as the changing from high salinity flooding formation brine to low salinity flooding of SW/10 for the non-fractured system. Reduction of endpoint water relative permeability gives an indication that the system is moving toward more water wetness. Similar findings were observed in the case of fractured cores, the optimum reduction of Krw $_{@S_{or}}$ is during SW/10 water flooding.
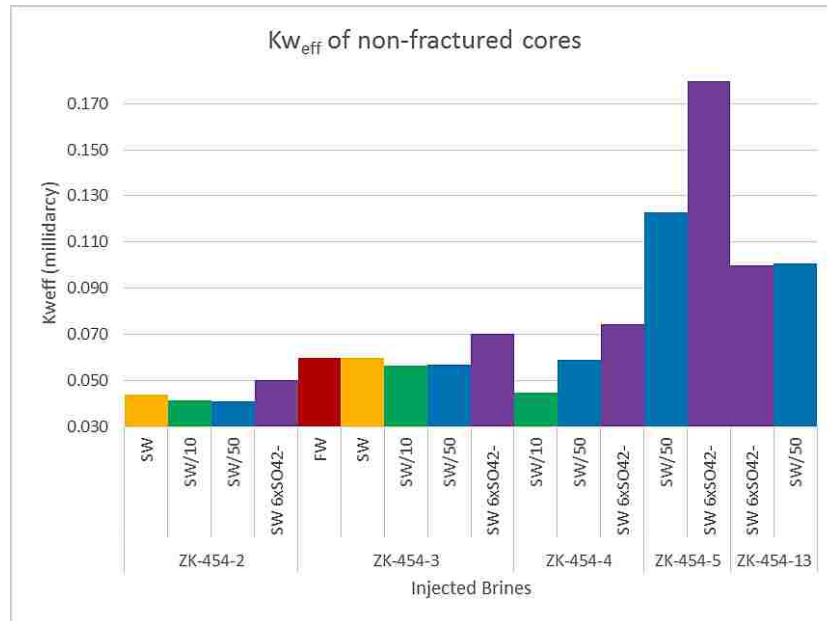
Figure 44: End point water relative permeability of secondary recovery non-fractured cores
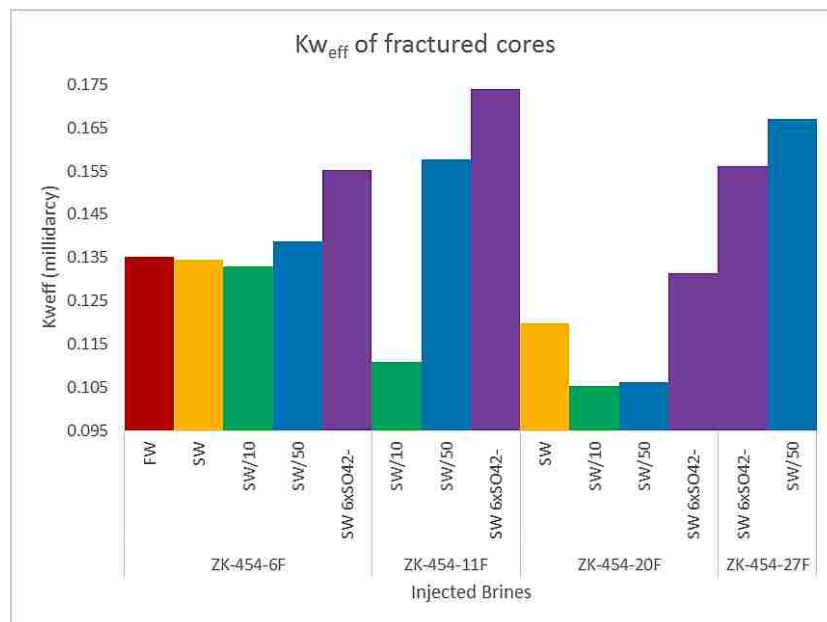
Figure 45: End point water relative permeability of secondary recovery fractured cores

A 27% reduction of Krw $_{@S_{or}}$ was estimated as the changing from high salinity flooding formation brine to low salinity flooding of SW/10 for the fractured system.

From all the sequential coreflooding tests (Figure 46), it is clear that combination of starting water using SW/10 and fracturing technique gives the best oil recovery of OOIP.
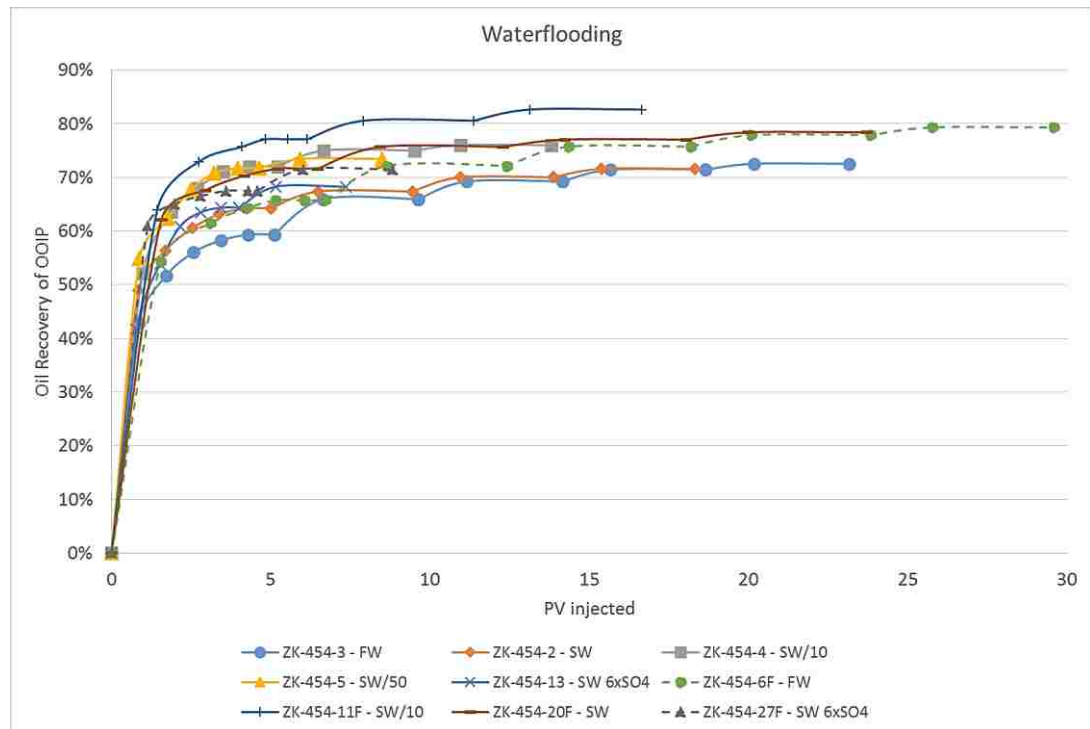
Figure 46: All results of coreflooding tests

Chapter 4: Conclusions and Recommendation for Future Works

Based on the results of the experimental work presented in this work, the following conclusions can be drawn:

1. From 5 sequential selected brines, SW/10 (6,252 ppm) is the optimum salinity by resulting the highest RF for both fractured and non-fractured cores, followed by SW/50, SW $6xSO_4^{-2}$, SW, and FW.

2. Wettability alteration that caused by fines migration and dissolution is the reason behind the improvement of low salinity water flooding as indicated by reducing water relative permeability and pressure drops during the flooding.

3. To minimize the operational cost and simplify the flooding process, the optimum system for oil recovery of low permeability oil reservoirs is SW/10 (6252 ppm) salinity system.

4. Fracturing the LPCR can improve oil recovery significantly for both high and low salinity water flooding.

5. Economic analysis should be conducted to compare with different schemes of fracturing and non-fracturing oil reservoirs.

Recommended for future works:

1. The additional waterflooding experiment is suggested, specifically dilution between SW/10 and SW/50.

2. Sulfate spiking 6 times in SW injected is not the best composition for selected reservoir condition. Less or more sulfate composition on the SW should be tested in order to get the best sulfate concentration in the injected water.

3. Contact angle and interfacial tension analysis could be done for selected reservoir condition to investigate in details the mechanism of LSWF.

4. Fracture density, ratio, and orientation should be studied as another variable to have a complete explanation of the effect of the fracturing system.

References

Abdallah, W., Buckley J. S., Carnegie, A., Edwards J., Herold, B., Fordham, E., Graue. A., Habashy, T., Seleznev N., Signer, C., Hussain, H., Montaron B., & Ziauddin, M. (2007). Fundamentals of Wettability (Oilfield Review of Schlumberger). Accessed on August 11, 2017, from http://www.slb.com/resources/publications/industry_articles/oilfield_review/2007/or2007sum04wettability.aspx

Ahmed, T. (2000). *Reservoir Engineering Handbook*. Gulf Publishing Company, Houston. Texas.

Al-Attar, H. H., Mahmoud, M. Y., Zekri. A. Y., AImehaideb, R., & Ghannam, M. (2013). Low-salinity flooding in a selected carbonate reservoir: experimental approach. *Journal of Petroleum Exploration and Production Technology*, 3(2), 139-149. Retrieved August 13, 2017 from https://doi.org/l0.l007/s13202-013 - 0052-3.

Al-Harrasi, A., Al-maamari, R. S., & Masalmeh, S. K. (2012). Laboratory Investigation of Low Salinity Waterflooding for Carbonate Reservoirs. Presented at Abu Dhabi International Petroleum Conference and Exhibition. SPE-161468-MS, 1620-1631. Retrieved August 12, 2017 from http://doi.org/lO.2118/l61468-MS.

Al-Quraishi, A. A., Al Hussinan, S. N., & Al Yami, H. Q. (2015). Efficiency and recovery mechanisms of low salinity waterflooding in sandstone and carbonate reservoir. Presented at Offshore Mediterranean Conference and Exhibition, OMC-2015-223, 1-14. Retrieved August 22, 2017 from https://www.onepetro.org/conference-paper/OMC-2015-223.

Alameri, W., Teklu, T. W., Graves, R. M., Kazemi, H. & Al Sumaiti A. M. (2015). Experimental and Numerical Modeling of Low-Salinity Waterflood in a Low Permeability Carbonate Reservoir. Presented at SPE Western regional Meeting, USA. Paper SPE-174001-MS, 1-16. Retrieved August 21, 2017 from https://doi.org/10.2118/174001-MS.

Alotaibi, M. B., Azmy, R., & Nasr-EI-Din, H. A. (2010). Wettability Challenges in Carbonate Reservoirs. Presented at the SPE Improved Oil Recovery Symposium USA. SPE-129972-MS, 1-20. Retrieved August 21, 2017 from https://doi.org/l0.21181/129972-MS.

Anderson, W. G. (1987). Wettability Literature Survey Part 5: The Effects of Wettability on Relative Permeability. SPE. *Journal of Petroleum Technology*. Volume 39, Issue 11, 1452-1468. Retrieved August 20, 2017 from https://doi.org/10.2118/16323-PA.

Austad, T., Rezaei Doust, A. & Puntervold, T. (2010). Chemical Mechanism of Low Salinity Water Flooding in Sandstone Reservoirs. Presented at the SPE Improved Oil Recovery Symposium USA. SPE129767, 1-17. Retrieved August 21, 2017 from https://doi.org/10.2118/129767-MS.

Bagci, S., Kok, M. V., & Turksoy. U. (2001). Effect of Brine Composition On Oil Recovery By Waterflooding. *Journal of Petroleum Science and Technology*, 19 (3-4), 359-372. Retrieved August 17, 2017 from https://doi.org/10.1081/LFT-100000769.

Ban, J., Arellano, J. L., Alawami, A., Aguilera, R. F., & Tallett, M. (2016). *World Oil Outlook*. Organization of the Petroleum Exporting Countries.

El-Dessouky, H. T. & Ettouney, H. M. (2002). *Fundamentals of Sea Water Desalination*. El Sevier, Amsterdam.

Jadhunandan, P., Morrow, N.R. (1995). Effect of Wettability on Waterflood Recovery for Crude Oil/Brine/Rock Systems. Society of Petroleum Engineers RE, 40–46. Retrieved August 14, 2017 from https://doi.org/10.2118/22597-PA

Kazankapov, N. (2014). Enhanced Oil Recovery in Caspian Carbonates With SmartWater. *Proceedings of the SPE Russian Oil and Gas Exploration and Production Technical Conference and Exhibition*. vol. SPE-171258-MS, 1097–1113. Retrieved August 24, 2017 from https://doi.org/10.2118/171258-RU.

Kilybay, A., Ghosh, B., & Thomas, N. C. (2017). A Review on the Progress of Ion-Engineered Water Flooding. *Journal of Petroleum Engineering*, Volume 2017, Article ID 7171957, 1-9. Retrieved August 18, 2017 from https://doi.org/10.1155/2017/7171957.

Morrow, N.R. (1990). Wettability and Its Effect on Oil Recovery. *Journal Petroleum Technology*, Volume 42, Issue 12, 1476-1484. Retrieved August 10, 2017 from https://doi.org/10.2118/21621-PA.

Nelson. R. A. (2001). *Geologic Analysis of Naturally Fractured Reservoirs*. Gulf Publishing Company, Houston. Texas.

Sheng, J. J. (2014). Critical Review of Low Salinity Water Flooding. *Journal of Petroleum Science and Engineering*. 120, 216-224. Retrieved August 13, 2017 from http://doi.org/ l0.1016/j.petrol.2014.05.026.

Speight, J. G. (2016). *Handbook of Hydraulic Fracturing*. New Jersey, John Wiley & Sons, Inc.

Stosur, G. J., Hite, J. R., Camahan, N. F., & Miller K. (2013). The Alphabet Soup of IOR, EOR and AOR: Effective Communication Requires a Definition of

Terms. Presented in SPE International Improved Oil Recovery Conference in Asia Pacific. SPE-84908-MS, 1-3. Retrieved August 10, 2017 from https://doi.org/10.2118/84908-MS.

Tadros, Th. F. (1987). *Solid-Liquid Dispersions*. Academic Press, London, United Kingdom.

Tang, G. Q., and Morrow, N. R. (1997). Salinity, Temperature, Oil Composition, and Oil Recovery by Waterflooding. SPE Reservoir Engineering. SPE-36680-PA, Volume 12, 269–276. Retrieved August 20, 2017 from https://doi.org/10.2118/36680-PA.

Tang, G. Q. & Morrow, N.R. (1999). Influence of Brine Composition and Fines Migration on Crude/Oil/Rock Interactions and Oil Recovery. *Journal Petroleum Science Engineering*, Volume 24, Issue 2-4, 99–111. Retrieved August 12, 2017 from https://doi.org/10.1016/S0920-4105(99)00034-0.

Teklu, T. W., Alameri W., Kazemi, H., Graves, R. M., AlSumaiti, A. M. (2014). Low-salinity Water-alternating-CO_2 Flooding Enhanced Oil Recovery: Theory and Experiments. Presented at the Abu Dhabi International Petroleum Exhibition and Conference. SPE 171767, 1-24. Retrieved August 12, 2017 from https://doi.org/10.2118/171767-MS.

Tip of the Mitt Watershed Council. (2013). What is Hydraulic Fracturing? Accessed on August 23, 2017, from http://www.watershedcouncil.org/learn/hydraulic-fracturing/.

Wu, Y. S. & Bai, B. (2009). Efficient Simulation for Low Salinity Waterflooding in Porous and Fractured Reservoirs. Presented at the SPE Reservoir Simulation Symposium USA. SPE118830, 1-13. Retrieved August 24, 2017 from https://doi.org/10.2118/118830-MS.

Yi, Z., & Sarma, H. K. (2012). Improving waterflood recovery efficiency in carbonate reservoirs through salinity variations and ionic exchanges: a promising low-cost 'Smart-Waterflood' approach. Presented at Abu Dhabi International Petroleum Conference and Exhibition. SPE-161631-MS, 1-21. Retrieved August 24, 2017. Retrieved August 9, 2017 from https://doi.org/10.2118/161631-MS.

Zahid, A., Shapiro, A. A., & Skauge, A. (2012). Experimental Studies of Low Salinity Waterflooding Carbonate: A New Promising Approach. *Proceedings of the SPE EOR Conference at Oil and Gas West Asia*. SPE-155625-MS, 835-848. Retrieved August 23, 2017, from https://doi.org/10.2118/155625-MS.

Zekri, A. Y., Nasr, M. S., & Al-Arabai. Z. I. (2011). Effect of LoSal on Wettability and Oil Recovery of Carbonate and Sandstone Format ion. Presented at

International Petroleum Technology Conference. IPTC-14131-MS, 1-11. Retrieved August 13, 2017 from https://doi.orgI l0.2523/IPTC-14131-MS.

Appendix A: Brine Preparation

All injected water's ionic composition that been used for the study were measured and reported by ADNOC using ICP (anions) and Ion chromatography (for cations). Ionic balance calculations were attempted to balance the brine compositions prior to brine preparations. The balancing was done using addition or subtraction of either Sodium or Chlorine ions, as they have proven to be non-determining ions in wettability alteration (Alotaibi et al., 2010). Regression analysis was used in calculations to achieve the "perfect" ionic balance value of 1.0. Table A.1 shows the example calculation for seawater:

Table A.1: An example of seawater ionic balance calculation.

Cations Analysed (mg/L)		Anions Analysed (mg/L)	
Na+	19054	Cl-	35835.77
Ca++	690	SO4-	3944
Mg++	2132	HCO3-	123
K+	672	CO3-	
Ba++		OH3-	
Fe++		I-	
Sr++		NO3-	
Li+		Br-	

Cations Analysed (meq/L)		Anions Analysed (meq/L)	
Na+	0.8288	Cl-	1.0108
Ca++	0.0344	SO4-	0.0411
Mg++	0.1754	HCO3-	0.002
K+	0.0172	CO3-	
Ba++		OH3-	
Fe++		I-	
Sr++		NO3-	0.0002
Li+		Br-	
Sum	1.06	Sum	1.06
Ratio of Cations to Anions			1

Comparison

The required amount of salts to prepare the brine with the specific ionic compositions was then calculated using a software developed by Core Laboratories International. The order of salts added was starting with divalent less electronegative ions and ending with NaCl.

Table A.2 shows an example calculations of salts required for seawater preparation.

Well	Field	Formation	Location	Wt. Of 10.078 cc Brine	Concentration(ppm)	Specific Gravity (gm/cc)
SB-0567	Asab	-	UAE	10.47891	60061	1.0398

Chemicals	Miligram/Litre	Gram/Litre	Gram/2 Litre	Order of Mixing
NaHCO3 (Anhy)	169.35	0.17	0.34	5
Na2CO3 (Anhy)	0	0	0	
Na2SO4 (Anhy)	5831.99	5.83	11.66	3
NaCl	43520.06	43.52	87.04	6
CaCl2 (Anhydrous)	1910.68	1.91	3.82	
CaCl2 2 H2O	2530.99	2.53	5.06	2
MgCl2.6H2O	17833.33	17.83	35.67	1
KCl	1281.3	1.28	2.56	4
SrCl2.6H2O	0	0	0	
LiCl	0	0	0	
BaCl2.2H2O	0	0	0	
CaCl2 6 H2O	3771.54	3.77	7.54	

The following procedure has been used for the preparation of brine:

1. Prepare a clean volumetric flask with the required volume 1, 2 or 5 liters.

2. Fill half of the volumetric flask (approximately) with deionized water.

3. Carefully place a magnetic stirrer in the flask and place the flask on the stirring pad and switch it on.

4. Add the required amount of salts following the orders on the excel spreadsheet.

5. Fill the volumetric flask to the required volume of 1, 2 or 5 liters (taking the volume of the stirrer into account).

6. Keep stirring until all the salts are dissolved.

7. Gently pour the brine in the side-arm flask and apply sufficient vacuum pressure (to remove dissolved gas in the brine) through side-arm of the flask and the stirrer is on.

8. When brine is completely transferred place a rubber bung on top of the side-arm flask. Turn both the vacuum and stirrer on for 2-3 minutes.

9. Measure the density and viscosity of the prepared brine using a Pycnometer and Canon-Fenske respectively.

10. Pour the prepared brine in a sealed container and label it accordingly.

Appendix B: Dilution and Sulfate Spiking

Dilution

All the diluted waters were prepared using seawater as the base water of the dilution. The calculations were done using the dilution equation as follows:

$$C_1 V_1 = C_2 V_2$$

Where:

C_1 = concentration of the sea water (ppm).

V_1 = required volume of seawater (ml).

C_2 = required concentration of the new solution (ppm).

V_2 = required volume of the new water (ml).

Sulfate Spiking

The spiking was done by adding of sodium sulphate (Na_2SO_4) salt. Although the addition of sulfate in the form of sodium sulfate increases the amount of sodium in the solution, this increase was insignificant as sulfate has proven to be a non-determining ion in wettability alteration (Alotaibi et al. 2010). Six-time spikings were selected as showed the better results at previous ADNOC research for Asab Field. The brine prepared based on the 885 mg/L of sulfate available in the formation water. Six-time sulfate spiking means that the concentration of sulfate in the brine is increased by 5,310 mg/L of sulfate ion. Six-time spiking was achieved by the addition of 7,854 grams of sodium sulfate into the original solution.

Appendix C: Core Preparation

Core Cleaning and Drying

A soxhlet extraction apparatus is used to extract the oil/brine from the core samples. In this method, toluene is gently boiled from a Pyrex flask; the vapor of toluene moves upward and condenses. The core plug is then submerged in the condensed toluene. When the level of the condensed fluid reaches the top of the siphon tune arrangement, the condensed toluene inside the soxhlet tube are automatically emptied to the boiling flask (using siphon effect).

All core samples were kept in toluene (to extract the oil) and methanol (to extract the brine and salts). The cleaning is continued until not traces of oil can be observed under the UV light. The following procedure is used for core cleaning with soxthlet apparatus.

1. Core sample is placed in the soxhlet.

2. Soxhlet is then connected to the boiling flask.

3. The extracting fluid is poured into the soxhlet until the siphon level (this is repeated for at least 3 times/cycles).

4. Connect the soxhlet to the condenser and make sure the water is running through the condenser.

5. Place the set-up on the heating mantle and provide enough heat until a proper condensation rate is achieved.

6. Stop the soxhlet when the core is completely clean and no extra fluid can be extracted (usually after a duration of 7 to 10) days.

7. Place the cores in the oven at a temperature of 150°C degrees for 2 to 3 days and take the measurement of dry weight for each core samples.

Core Fracturing

An artificial fracture was created perpendicularly with the length of 4 core samples to modify the permeability and create a flow path through the core. The following procedure is used for fracturing the cores.

1. Core samples are measured to make the slabbing point target

2. Core is placed on the core slab machine.

3. Switch on the machine and slab the cores prepared equally.

4. Once the core been slabbed, place some aluminium foil paper in between 2 slabbed cores.

5. Aluminium foil paper has the same size with length and diameter of core. These paper will keep the fracture be opened.

6. Combine 2 slabbed cores with the paper in between to be formed as a single core.

7. Cover the outer part of the core with aluminum paper and apply some glue to make the aluminium foil attached.

8. Wait for a while until the cores are stable.

9. Fractured cores ready to be used.

Core Saturation

A method which is a combination of vacuum and pressure is used to saturate the core plugs with the formation brine.

Vacuuming

In this stage of saturation experiment, vacuum pressure is used to empty the air from the pore space of the core plug.

1. In order to use less volume of formation water, fill half the saturation cylinder with core plugs that won't be used in the study.

2. Cover the cores with the formation brine completely.

3. Lay the cores that are to be saturated, on the cores that are used to fill the dead volume of the cylinder. Make sure that the cores are dry and completely out of the brine

4. Put the lid of the chamber and close prefilling and pressure valves.

5. Open the vacuum valve, connect it to the vacuum stream and let it run over night.

2. Pressurizing

After applying the vacuum pressure for an overnight, the chamber is completely filled and pressurized with formation brine. The following is the procedure used for pressurizing the core plugs with formation water.

1. Close the vacuum valve and pressure valve.

2. Put the prefilling source in the container filled with enough brine and then open the prefilling valve.

3. Wait for 20-30 minutes for the chamber to get filled with its original vacuum pressure

Note: that this pressure of -1atm is only enough to saturate the larger pores of the core. In order to saturate the pores with very small radius, it is needed to increase the pressure of the chamber to approximately 3000 psi. Capillary pressure equation shows that in order to fill pores with small radiuses, it is needed to impose high pressures. To pressurize the cell the injection pump was used:

4. Close the "outlet" valve and open the "inlet" valve

5. Press "RUN" to empty the storage chamber of the injection pump from distilled water

6. Put the outlet or "refilling" line in the brine bottle (or container) and press "REFILL", until you see a message on the screen saying "REFILLING COMPLETE".

7. Close the "inlet" valve and open the "outlet" Valve

8. Connect the outlet of the injection pump to the pressure valve of the saturator.

9. Close all the valves of the saturator and open pressure valve.

10. Choose one of the "constant pressure" or "constant flowrate" methods and set your pressure or flow rate accordingly.

11. Press run to fill and pressurize the saturator chamber to the required pressure of 3000 psig.

12. It is recommended to:

Up to 2700 psig with 25 cc/min.

Up to 3000 psig with constant pressure.

13. Once the pressure of 3000 psig is achieved, close the pressure valve of the saturator

and let it stay under high pressure for a day.

14. Empty the cylinder of the injection pump and refill it with DI water.

Once the cores saturated by water, Pore Volume (PV) and Porosity of cores by

water could be measured using following equations:

$$PV = \frac{Wsaturated - Wdry}{\rho\ water}$$

$$\emptyset water = \frac{PV}{Vbulk}$$

Where:

PV : Volume of pores connected and filled with water (cc).

$Wsaturated$: Weight of core after fully saturated with water.

$Wdry$: Weight of dry core.

$\emptyset water$: Total percentage volume of pore by volume total of core.

$Vbulk$: Volume total of core.

Appendix D: Porosity and Permeability Measurement

Porosity and Permeability Measurements Using Nitrogen Gas

The Vinci PoroPerm Instrument is used to measure the density, porosity and permeability of the core sample using nitrogen gas.

Porosity Measurement: The ideal gas law is used to calculate the pore volume and eventually, the grain density. A cell with a known volume is first filled with nitrogen gas and the pressure is recorded as Pref. It is then connected to another cell containing the core plug, with an unknown volume" (pore volume). The new pressure is measured as Pexp and is used to find the unknown volume (pore volume). The procedures to measure porosity is as follows:

1. Connect the plastic pressure input to the nitrogen gas cylinder.

2. Gently open the valve on the nitrogen cylinder until a pressure of approximately 150 psia is read on the gauge. Do not apply any confining pressure (confining pressure valve should be on Vent).

3. Click on "Update Patm" to update and recalibrate the pressure sensors.

4. Place the core sample into the cell and fill the gap with the provided billets.

5. Select "GV+PV" and "No permeability measurement.

6. The only two valves used during Porosity measurements are Source valve and

Matrix valve:

a. Source valve should always be "ON".

b. Matrix valve is opened/closed during the test.

7. Keep the cell separated.

8. Input the following information into the software:

Report name, Operator name, Sample name, Weight (gram), Diameter (mm), Length (mm), Sample #, Number of billets used.

9. Press "START": Grain volume is calculated based on the dimensions.

10. Press "YES" (after checking the TO DO list): The first cell is filled with gas (pressure build up) and the cell pressure is then reported as "Pre".

11. Turn the MATRIX CUP valve to "pressure" and press "OK".

12. Turn the MATRIX CUP valve to "Vent" and press "OK".

Pexp is then stabilized and recorded to calculate pore volume and grain density.

Permeability measurements: The PoroPerm instrument can also be used to measure the permeability of a core sample using nitrogen gas. The software provided by Vinci Company has a built-in function to accounts for the slippage and Klinkenberg effects, and corrects the permeability values automatically. The procedure to measure permeability is as follows:

1. Connect the pressure input of the instrument to the gas cylinder and apply a confining pressure of 350-400 psia.

2. Select "No Volume Measurement" and "Kg Autoflow" on the screen.

3. The only valve used during permeability measurements is the "Confining Pressure" valve. The position of other valves should always be as:

a. Source valve should be "ON".

b. Matrix valve on "VENT".

c. Flow valve on "FPRWARD".

4. Click on "Update Patm" to update and recalibrate the pressures sensors.

5. Input the followings into the software:

Report name, Operator name, Sample name, Diameter (mm), Length (mm), Sample #.

6 Load the core plug in the cell and close it tightly.

7 Open the inlet and outlet valves.

8 Apply the confining pressure of 350-400 psi by turning the "CONFINING PRESSURE" valve to "PRESSURE".

9 Press "START", an excel spreadsheet will open and the dimensions and data will be recorded.

10 Press "YES" (after checking the TO DO list).The flow starts and it is scanned automatically each 15-30 seconds.

11 The software will report the calculated K value when it has stabilized.

Permeability Measurements Using Water Flooding

Core-holder and the core-flooding apparatus can be utilized to:Measure the absolute permeability by injecting brine in a core sample of fully saturated brine (Sw of 100%). Measure the recovery factor for various secondary/tertiary oil recovery techniques, Construct the relative permeability curves, etc..

Permeability measurements: The procedure used for measurement of absolute permeability is as follows:

1. Gently place the core sample (at Sw of 100%) in the sleeve.

2. Place the flood head at one end and the end-stem at the other end of the core.

3. Lubricate the end-stem with some hydraulic oil and place the above set-up into the core holder gently (to save time, you can also pure about 10 ml of hydraulic oil in the core holder before loading the set-up).

4. Tightly close the the cap of the core holder.

5. Apply overburden pressure of 800 PSI.

6. Connect the injection pump to one inlet of the flood-head and start the injection at a constant flow rate of 2cc/min.

7. Close the second inlet on the flood-head after you observe the water coming out of the second inlet. This is to bleed-off the air in the core holder.

8. Observe the injection pressure on the screen of the injection pump and report it when it stabilizes.

9. Stop the injection pump.

10. Unload the core sample.

11. Release the overburden pressure by opening the valve on the hydraulic pump.

12. Open both inlets of the flood head then open the cap.

13. To remove the sleeve along with the flood-head and end-stem, close the valve on the overburden pressure pump and pump some hydraulic oil into the core holder The absolute permeability to the liquid is then measured as:

$$K = \frac{14700 \times Q \ \times \mu \times L}{A \times \Delta P}$$

Where:

Q: Injection rate (ml/sec).

μ: Viscosity of the injection fluid (cP).

L: Length of the core (cm).

A: Cross-Sectional area of the core (m^2).

ΔP: Pressure across the core (psi).

Appendix E: Core Flooding

Oilflooding

After brine saturation, all cores are flooded with the reservoir oil until no more formation brine is produced. At the end of the core flooding experiment, core plugs are at the initial water saturation (Swi) conditions.

The procedure for the oil flooding experiments is similar to the procedure explained for permeability measurement using water (Appendix E). Core flooding is conducted using the following procedure. Only differences between water-flooding and oil-flooding experiments are:

1. Gently place the core sample (at Sw of 100%) in the rubber sleeve.

2. Place the flood head at one end and the end-stem at the other end of the core.

3. Lubricate the end-stem with some hydraulic oil and place the sleeve into the core holder gently.

4. Tightly close the Cap of the core holder and apply overburden pressure of 800 PSI.

5. Connect a pressure regulator valve to the end-stem. Keep the back pressure valve closed completely.

6. Connect the oil container at the back of the core holder to the nitrogen cylinder and apply a pressure of 400 psig and connect the outlet of the pressurized oil container to one inlet of the flood-head.

7. Close the second inlet on the flood-head after you observe the water coming out of the second inlet. This is to bleed-off the air in the core holder.

8. Open the oil injection valve completely while the regulator valve on the end-stem is still closed. This is to build up the pressure inside the core and ensure the flow stability.

9. Gently open the back pressure valve until a proper production rate (approximately one drop of effluent every 3 seconds) is obtained.

10. Collect the produced effluents and report the cumulative volume of the produced brine and continue the oil flood until no more brine is produced.

11. Stop the injection pump, unload the core sample, and elease the overburden pressure by opening the valve on the hydraulic pump.

12. Open both inlets of the flood head then open the cap of the core holder.

13. To remove the sleeve along with the flood-head and end-stem, close the valve on the overburden pressure pump and pump some hydraulic oil into the core holder.

The initial water saturation of the core plug is calculated as:

$$Swi = \frac{PV - Vwater}{PV}$$

$$Soi = 1 - Swi$$

Where

PV is the pore volume calculated using saturated weight of the core sample (Appendix D).

Vwater is the cumulative volume of the produced brine at the end of oil flooding experiment (Table 7).

Swi is the initial water saturation (Table 7).

Soi is the initial oil saturation (Table 7).

Oil flooding experiment is usually reconducted after aging of the core plugs to alteration due to aging. Producing more water after aging would mean that the wettability of the rock has moved toward a more oil-wetting state evaluate any wettability.

Low Salinity Water Flooding Experiments

The aged core plugs were being flooded with various brines to evaluate the effect of dilution and sulfate spiking on oil recovery. The low salinity water flooding experiments were all conducted at reservoir temperature of 90°C. LSWF experiments are conducted using the following procedure.

1. Gently place the aged core sample (in So) in the rubber sleeve.

2. Place the flood head at one end and the end-stem at the other end of the core.

3. Lubricate the end-stem with some hydraulic oil and place the sleeve alone with the flood head and end-stem into the core holder gently.

4. Tightly close the cap of the core holder.

5. Apply overburden pressure of 800 PSI.

6. Adjust the back pressure regulator valve to a pressure of 100 psia, and connect to the end-stem.

7. Wrap the core holder with the heating tape and cover it with aluminum foil.

8. Increase the temperature of the core holder stepwise (steps of 20 °C).

9. Fill the injection pump with the injected brine (as explained in Appendix A).

10. Connect outlet of the injection pump to one inlet of the flood-head.

11. Close the second inlet on the flood-head after you observe the water coming out of the second inlet. This is to bleed-off the air in the core holder.

12. Operate the injection pump at the constant injection rate of 1 cc/min.

13. Collect the produced effluents and report the time, the pressure and the volume of the produced oil.

14. Continue the oil flood until no more brine is produced.

15. Stop the injection pump.

16. Empty and refill the pump with the next injection brine (if any).

17. Continue the flooding with the next brine at the same injection rate of 1 cc/min.

18. Stop the flooding experiment when no more oil in produced.

19. Unload the core sample.

20. Release the overburden pressure by opening the valve on the hydraulic pump.

21. Open both inlets of the flood head then open the cap of the core holder.

22. To remove the sleeve along with the flood-head and end-stem, close the valve on the overburden pressure pump and pump some hydraulic oil into the core holder. For every pore volume injected, the recovery factor (RF) is calculated as:

$$RF = \frac{Voi - Vop}{Voi}$$

Where

Voi is the volume of oil initially in place.

Vop is the cumulative volume of the oil produced at a specific pore volume injected.

Appendix F: Effluent water analysis

After waterflooding tests, Effluent water will be tested for the salinity, resistivity, conductivity, and pH. Comparison between properties of water before and after flooding may give the information about the underlying mechanism behind LSWF process.

Digital resistivity meter

Resistivity and salinity of brines were measured using a digital resistivity manufactured by OFITE. The measurement was conducted using the following procedure.

1.   Press the "Power/Exit" button to turn the unit on. The display screen will show the temperature and either Resistivity or Concentration of NaCl.

2.   Use the suction bulb to pull the sample into the lucite cell. Empty and refill the cell several times to thoroughly wet the cylinder walls.

3.   Connect the cell to the two terminal posts on the meter. Be sure the sample fills the area between the two metal posts in the cell. Wait for the sample to reach room temperature.

4.   Record the Resistivity/Concentration and Temperature from the display screen.

Conductivity and pH meter

Conductivity and pH of water were measured using a digital conductivity meter and pH meter manufactured by HACH. The measurement was conducted using the following procedure.

1.   Switch on the conductivity/ph meter.

2.   Make sure the tool is been calibrated.

3.   Place the probe into the water sample and wait until the measuring process been stable.

4.   Read the measurement.

5.   Clean the probe before doing the measurement for next water.

TDS calculation

Total Dissolved Solid (TDS) was calculated using a program developed by Chemiasoft. It is converting the salinity of water to TDS using Standard Methods for the Examination of Water and Wastewater, 20th edition, 1999. The program could be accessed on http://www.chemiasoft.com/chemd/TDS.

Appendix G: Plotted Data

ZK-454-2

No.	Injected Brines	Voil Produced (cc)	Vwater Injected (cc)	Incremental RF (%)	RF (%)	Incremental PV injected	PV injected
1	SW	0	0	0.000	0.000	0.000	0.000
		4.65	5.4	48.947	48.947	0.846	0.846
		0.7	9.3	7.368	56.316	0.846	1.692
		0.4	9.6	4.211	60.526	0.846	2.538
		0.25	9.8	2.632	63.158	0.846	3.385
		0.1	10.0	1.053	64.211	0.855	4.239
		0	9.0	0.000	64.211	0.762	5.001
2	SW/10	0.3	17.4	3.158	67.368	1.501	6.501
		0	34.9	0.000	67.368	2.950	9.452
3	SW/50	0.25	17.4	2.632	70.000	1.496	10.948
		0	34.7	0.000	70.000	2.933	13.881
4	SW 6xSO4^{-2}	0.15	17.4	1.579	71.579	1.488	15.369
		0	35.0	0.000	71.579	2.959	18.328

Injected Brines	No.	Vwater Injected (cc)	Cummulative Vwater Injected (cc)	PV injected	Δ Pressure (psi)	dP/dPmax	PV injected
						0.000	0.000
						0.902	0.714
SW	1	0.000	0.000	0.000	0	0.998	1.429
	2	8.443	8.443	0.714	1150	1.000	2.143
	3	8.443	16.886	1.429	1273	0.996	2.858
	4	8.443	25.329	2.143	1275	0.998	3.572
	5	8.443	33.771	2.858	1270		
	6	8.443	42.214	3.572	1272	0.991	4.286
	7	8.443	50.657	4.286	1264	0.980	5.001
	8	8.443	59.100	5.001	1250	0.941	5.637
SW/10	1	7.514	66.614	5.637	1200	0.933	6.272
	2	7.514	74.129	6.272	1190	0.882	6.908
	3	7.514	81.643	6.908	1125	0.900	7.544
	4	7.514	89.157	7.544	1147	0.899	8.180
	5	7.514	96.671	8.180	1146	0.894	8.816
	6	7.514	104.186	8.816	1140	0.891	9.452
	7	7.514	111.700	9.452	1136	0.902	10.928
SW/50	1	17.450	129.150	10.928	1150	0.888	12.405
	2	17.450	146.600	12.405	1132	0.875	13.881
	3	17.450	164.050	13.881	1115	0.863	15.363
SW 6xSO42-	1	17.517	181.567	15.363	1100	0.884	16.846
	2	17.517	199.083	16.846	1127	0.878	18.328
	3	17.517	216.600	18.328	1120		

ZK-454-4

No.	Injected Brines	Voil Produced (cc)	Vwater Injected (cc)	Incremental RF (%)	RF (%)	Incremental PV injected	PV injected
1	SW/10	0	0	0.000	0.000	0.000	0.000
		5.2	6.8	52.000	52.000	0.980	0.980
		1.15	9.9	11.500	63.500	0.898	1.878
		0.45	9.6	4.500	68.000	0.817	2.695
		0.3	9.7	3.000	71.000	0.817	3.512
		0.1	9.9	1.000	72.000	0.817	4.329
		0	11.0	0.000	72.000	0.898	5.227
2	SW/50	0.3	17.4	3.000	75.000	1.446	6.673
		0	34.8	0.000	75.000	2.842	9.515
3	SW 6xSO4^{-2}	0.1	17.5	1.000	76.000	1.435	10.950
		0	34.9	0.000	76.000	2.853	13.803

Injected Brines	No.	Vwater Injected (cc)	Cummulative Vwater Injected (cc)	PV injected	Δ Pressure (psi)	dP/dPmax	PV injected
						0.000	0.000
SW/10	1	0.000	0.000	0.000	0	0.966	0.653
	2	8.000	8.000	0.653	1700	1.000	1.307
	3	8.000	16.000	1.307	1759	0.925	1.960
	4	8.000	24.000	1.960	1627	0.790	2.614
	5	8.000	32.000	2.614	1389	0.706	3.267
	6	8.000	40.000	3.267	1241	0.649	3.920
	7	8.000	48.000	3.920	1142	0.632	4.574
	8	8.000	56.000	4.574	1112	0.628	5.227
	9	8.000	64.000	5.227	1105	0.550	5.942
SW/50	1	8.750	72.750	5.942	968	0.526	6.656
	2	8.750	81.500	6.656	925	0.511	7.371
	3	8.750	90.250	7.371	899	0.500	8.086
	4	8.750	99.000	8.086	879	0.494	8.800
	5	8.750	107.750	8.800	869	0.461	9.515
	6	8.750	116.500	9.515	811	0.478	10.229
SW 6xSO42-	1	8.750	125.250	10.229	840	0.470	10.944
	2	8.750	134.000	10.944	826	0.464	11.659
	3	8.750	142.750	11.659	817	0.459	12.373
	4	8.750	151.500	12.373	807	0.452	13.088
	5	8.750	160.250	13.088	795	0.448	13.803
	6	8.750	169.000	13.803	788		

ZK-454-5

No.	Injected Brines	Voil Produced (cc)	Vwater Injected (cc)	Incremental RF (%)	RF (%)	Incremental PV injected	PV injected
1	SW/50	0	0	0.000	0.000	0.000	0.000
		6.2	5.8	54.867	54.867	0.881	0.881
		0.85	11.2	7.522	62.389	0.881	1.762
		0.6	9.4	5.310	67.699	0.734	2.496
		0.35	9.7	3.097	70.796	0.734	3.230
		0.1	9.9	0.885	71.681	0.734	3.964
		0	9.1	0.000	71.681	0.668	4.632
2	SW 6xSO4^{-2}	0.2	17.5	1.770	73.451	1.299	5.932
		0	35.0	0.000	73.451	2.569	8.501

Injected Brines	No.	Vwater Injected (cc)	Cummulative Vwater Injected (cc)	PV injected	Δ Pressure (psi)	dP/dPmax	PV injected
						0.000	0.000
SW/50	1	0.000	0.000	0.000	0	1.000	0.579
	2	7.888	7.888	0.579	610	0.967	1.158
	3	7.888	15.775	1.158	590	0.905	1.737
	4	7.888	23.663	1.737	552	0.836	2.316
	5	7.888	31.550	2.316	510	0.764	2.895
	6	7.888	39.438	2.895	466	0.730	3.474
	7	7.888	47.325	3.474	445	0.649	4.053
	8	7.888	55.213	4.053	396	0.625	4.632
	9	7.888	63.100	4.632	381	0.607	5.277
SW 6xSO42-	1	8.783	71.883	5.277	370	0.574	5.922
	2	8.783	80.667	5.922	350	0.593	6.567
	3	8.783	89.450	6.567	362	0.566	7.212
	4	8.783	98.233	7.212	345	0.530	7.856
	5	8.783	107.017	7.856	323	0.525	8.501
	6	8.783	115.800	8.501	320		

ZK-454-13

No.	Injected Brines	Voil Produced (cc)	Vwater Injected (cc)	Incremental RF (%)	RF (%)	Incremental PV injected	PV injected
1	SW 6xSO$_4^{-2}$	0	0	0.000	0.000	0.000	0.000
		4.8	7.6	41.739	41.739	0.790	0.790
		1.4	10.1	12.174	53.913	0.733	1.523
		0.8	9.2	6.957	60.870	0.637	2.161
		0.3	9.7	2.609	63.478	0.637	2.798
		0.1	9.9	0.870	64.348	0.637	3.436
		0	9.1	0.000	64.348	0.580	4.016
2	SW/50	0.45	17.4	3.913	68.261	1.137	5.153
		0	34.8	0.000	68.261	2.216	7.369

Injected Brines	No.	Vwater Injected (cc)	Cummulative Vwater Injected (cc)	PV injected	Δ Pressure (psi)	dP/dPmax	PV injected
						0.000	0.000
						0.906	0.502
SW 6xSO42-	1	0.000	0.000	0.000	0	1.000	1.004
	2	7.875	7.875	0.502	704	0.889	1.506
	3	7.875	15.750	1.004	777	0.815	2.008
	4	7.875	23.625	1.506	691	0.734	2.510
	5	7.875	31.500	2.008	633	0.723	3.012
	6	7.875	39.375	2.510	570	0.669	3.514
	7	7.875	47.250	3.012	562	0.660	4.016
	8	7.875	55.125	3.514	520	0.631	4.575
	9	7.875	63.000	4.016	513	0.611	5.133
SW/50	1	8.767	71.767	4.575	490	0.550	5.692
	2	8.767	80.533	5.133	475	0.550	6.251
	3	8.767	89.300	5.692	427	0.544	6.810
	4	8.767	98.067	6.251	427	0.534	7.369
	5	8.767	106.833	6.810	423		
	6	8.767	115.600	7.369	415		

ZK-454-27F

No.	Injected Brines	Voil Produced (cc)	Vwater Injected (cc)	Incremental RF (%)	RF (%)	Incremental PV injected	PV injected
1	SW 6xSO$_4^{-2}$	0	0	0.000	0.000	0.000	0.000
		6.1	8.0	61.000	61.000	1.136	1.136
		0.4	10.0	4.000	65.000	0.838	1.973
		0.15	10.0	1.500	66.500	0.817	2.791
		0.1	9.9	1.000	67.500	0.805	3.596
		0	8.5	0.000	67.500	0.685	4.281
		0	3.7	0.000	67.500	0.298	4.579
2	SW/50	0.4	17.4	4.000	71.500	1.436	6.015
		0	34.9	0.000	71.500	2.808	8.823

Injected Brines	No.	Vwater Injected (cc)	Cummulative Vwater Injected (cc)	PV injected	Δ Pressure (psi)	dP/dPmax	PV injected
						0.000	0.000
						1.000	0.572
SW 6xSO42-	1	0.000	0.000	0.000	0	0.824	1.145
	2	7.106	7.106	0.572	459	0.712	1.717
	3	7.106	14.213	1.145	378	0.678	2.289
	4	7.106	21.319	1.717	327	0.682	2.862
	5	7.106	28.425	2.289	311	0.654	3.434
	6	7.106	35.531	2.862	313	0.649	4.006
	7	7.106	42.638	3.434	300	0.651	4.579
	8	7.106	49.744	4.006	298	0.575	5.286
	9	7.106	56.850	4.579	299	0.532	5.993
SW/50	1	8.783	65.633	5.286	264	0.532	6.701
	2	8.783	74.417	5.993	244	0.508	7.408
	3	8.783	83.200	6.701	244	0.519	8.116
	4	8.783	91.983	7.408	233	0.497	8.823
	5	8.783	100.767	8.116	238		
	6	8.783	109.550	8.823	228		

ZK-454-11F

No.	Injected Brines	Voil Produced (cc)	Vwater Injected (cc)	Incremental RF (%)	RF (%)	Incremental PV injected	PV injected
1	SW/10	0	0	0.000	0.000	0.000	0.000
		4.6	9.6	63.889	63.889	1.436	1.436
		0.65	12.3	9.028	72.917	1.310	2.746
		0.2	13.2	2.778	75.694	1.355	4.101
		0.1	7.1	1.389	77.083	0.728	4.829
		0	7.0	0.000	77.083	0.708	5.537
		0	6.0	0.000	77.083	0.607	6.144
2	SW/50	0.25	17.2	3.472	80.556	1.761	7.905
		0	34.3	0.000	80.556	3.472	11.378
3	SW 6xSO4^{-2}	0.15	17.3	2.083	82.639	1.765	13.143
		0	34.6	0.000	82.639	3.499	16.642

Injected Brines	No.	Vwater Injected (cc)	Cummulative Vwater Injected (cc)	PV injected	Δ Pressure (psi)	dP/dPmax	PV injected
SW/10	1	0.000	0.000	0.000	0	0.000	0.000
	2	7.594	7.594	0.768	525	0.921	0.768
	3	7.594	15.188	1.536	570	1.000	1.536
	4	7.594	22.781	2.304	451	0.791	2.304
	5	7.594	30.375	3.072	386	0.677	3.072
	6	7.594	37.969	3.840	321	0.563	3.840
	7	7.594	45.563	4.608	341	0.598	4.608
	8	7.594	53.156	5.376	265	0.465	5.376
	9	7.594	60.750	6.144	289	0.507	6.144
SW/50	1	8.625	69.375	7.016	244	0.428	7.016
	2	8.625	78.000	7.889	237	0.416	7.889
	3	8.625	86.625	8.761	219	0.384	8.761
	4	8.625	95.250	9.633	214	0.375	9.633
	5	8.625	103.875	10.505	210	0.368	10.505
	6	8.625	112.500	11.378	197	0.346	11.378
SW 6xSO42-	1	8.675	121.175	12.255	244	0.428	12.255
	2	8.675	129.850	13.133	237	0.416	13.133
	3	8.675	138.525	14.010	254	0.446	14.010
	4	8.675	147.200	14.887	240	0.421	14.887
	5	8.675	155.875	15.765	231	0.405	15.765
	6	8.675	164.550	16.642	219	0.384	16.642

ZK-454-6F

No.	Injected Brines	Voil Produced (cc)	Vwater Injected (cc)	Incremental RF (%)	RF (%)	Incremental PV injected	PV injected
1	FW	0	0	0.000	0.000	0.000	0.000
		3.8	10.3	54.286	54.286	1.554	1.554
		0.5	13.7	7.143	61.429	1.565	3.118
		0.2	10.2	2.857	64.286	1.146	4.264
		0.1	8.1	1.429	65.714	0.904	5.168
		0	8.0	0.000	65.714	0.882	6.049
		0	6.0	0.000	65.714	0.661	6.711
2	SW	0.45	17.1	6.429	72.143	1.938	8.648
		0	34.3	0.000	72.143	3.776	12.424
3	SW/10	0.25	17.3	3.571	75.714	1.938	14.361
		0	34.7	0.000	75.714	3.820	18.181
4	SW/50	0.15	17.1	2.143	77.857	1.897	20.078
		0	34.1	0.000	77.857	3.761	23.840
5	SW 6xSO4^{-2}	0.1	17.3	1.429	79.286	1.921	25.761
		0	34.7	0.000	79.286	3.820	29.580

Injected Brines	No.	Vwater Injected (cc)	Cummulative Vwater Injected (cc)	PV injected	Δ Pressure (psi)	dP/dPmax	PV injected
						0.000	0.000
						1.000	0.959
FW	1	0.000	0.000	0.000	0	0.950	1.917
	2	8.700	8.700	0.959	544	0.930	2.876
	3	8.700	17.400	1.917	517	0.888	3.835
	4	8.700	26.100	2.876	506	0.811	4.793
	5	8.700	34.800	3.835	483	0.785	5.752
	6	8.700	43.500	4.793	441	0.759	6.711
	7	8.700	52.200	5.752	427	0.763	7.527
	8	8.700	60.900	6.711	413	0.695	8.343
SW	1	7.407	68.307	7.527	415	0.594	9.159
	2	7.407	75.714	8.343	378	0.579	9.975
	3	7.407	83.121	9.159	323	0.585	10.792
	4	7.407	90.529	9.975	315	0.592	11.608
	5	7.407	97.936	10.792	318	0.588	12.424
	6	7.407	105.343	11.608	322	0.572	13.383
	7	7.407	112.750	12.424	320	0.577	14.343
SW/10	1	8.708	121.458	13.383	311	0.542	15.303
	2	8.708	130.167	14.343	314	0.533	16.262
	3	8.708	138.875	15.303	295	0.533	17.222
	4	8.708	147.583	16.262	290	0.515	18.181
	5	8.708	156.292	17.222	290	0.529	19.124
	6	8.708	165.000	18.181	280	0.511	20.067
SW/50	1	8.558	173.558	19.124	288	0.509	21.010
	2	8.558	182.117	20.067	278	0.507	21.953
	3	8.558	190.675	21.010	277	0.498	22.897
	4	8.558	199.233	21.953	276	0.478	23.840
	5	8.558	207.792	22.897	271	0.463	24.988
	6	8.558	216.350	23.840	260	0.482	26.136
SW 6xSO4^{2-}	1	10.420	226.770	24.988	252	0.515	27.284
	2	10.420	237.190	26.136	262	0.526	28.432
	3	10.420	247.610	27.284	280	0.524	29.580
	4	10.420	258.030	28.432	286		
	5	10.420	268.450	29.580	285		

ZK-454-20F

No.	Injected Brines	Voil Produced (cc)	Vwater Injected (cc)	Incremental RF (%)	RF (%)	Incremental PV injected	PV injected
1	SW	0	0	0.000	0.000	0.000	0.000
		4.6	9.6	62.162	62.162	1.570	1.570
		0.4	12.0	5.405	67.568	1.371	2.941
		0.2	10.8	2.703	70.270	1.216	4.157
		0.1	9.6	1.351	71.622	1.072	5.230
		0	5.8	0.000	71.622	0.641	5.871
		0	5.5	0.000	71.622	0.608	6.479
2	SW/10	0.3	17.4	4.054	75.676	1.961	8.439
		0	34.9	0.000	75.676	3.855	12.294
3	SW/50	0.1	17.4	1.351	77.027	1.938	14.233
		0	34.5	0.000	77.027	3.811	18.043
4	SW 6xSO4^{-2}	0.1	17.4	1.351	78.378	1.938	19.982
		0	33.6	0.000	78.378	3.711	23.693

Injected Brines	No.	Vwater Injected (cc)	Cummulative Vwater Injected (cc)	PV injected	Δ Pressure (psi)	dP/dPmax	PV injected
						0.000	0.000
						1.000	0.926
SW	1	0.000	0.000	0.000	0	0.942	1.851
	2	8.371	8.371	0.926	565	0.802	2.777
	3	8.371	16.743	1.851	532	0.708	3.702
	4	8.371	25.114	2.777	453	0.701	4.628
	5	8.371	33.486	3.702	400	0.623	5.553
	6	8.371	41.857	4.628	396	0.554	6.479
	7	8.371	50.229	5.553	352	0.642	7.310
	8	8.371	58.600	6.479	313	0.586	8.140
SW/10	1	7.514	66.114	7.310	363	0.584	8.971
	2	7.514	73.629	8.140	331	0.598	9.802
	3	7.514	81.143	8.971	330	0.627	10.633
	4	7.514	88.657	9.802	338	0.545	11.464
	5	7.514	96.171	10.633	354	0.545	12.294
	6	7.514	103.686	11.464	308	0.515	14.211
	7	7.514	111.200	12.294	308	0.457	16.127
SW/50	1	17.333	128.533	14.211	291	0.524	18.043
	2	17.333	145.867	16.127	258	0.513	19.927
	3	17.333	163.200	18.043	296	0.519	21.810
SW 6xSO42-	4	17.033	180.233	19.927	290	0.519	23.693
	5	17.033	197.267	21.810	293		
	6	17.033	214.300	23.693	293		